NACA

RESEARCH MEMORANDUM

DOWNWASH CHARACTERISTICS AND VORTEX-SHEET SHAPE BEHIND

A 63° SWEPT-BACK WING-FUSELAGE COMBINATION

AT A REYNOLDS NUMBER OF 6.1×10^6

By William H. Tolhurst, Jr.

Ames Aeronautical Laboratory
Moffett Field, Calif.

NATIONAL ADVISORY COMMITTEE
FOR AERONAUTICS

WASHINGTON
December 15, 1952

NATIONAL ADVISORY COMMITTEE FOR AERONAUTICS

RESEARCH MEMORANDUM

DOWNWASH CHARACTERISTICS AND VORTEX-SHEET SHAPE BEHIND

A 63° SWEPT-BACK WING-FUSELAGE COMBINATION

AT A REYNOLDS NUMBER OF 6.1 × 10⁶

By William H. Tolhurst, Jr.

SUMMARY

An experimental investigation has been conducted to define the downwash field and vortex-sheet shape behind a wing-fuselage combination incorporating a 63° swept-back wing of aspect ratio 3.5. Data for nine vertical transverse planes located between 0.57 and 2.71 semispans behind the 0.25 mean aerodynamic chord point are presented for three angles of attack at a Reynolds number of 6.1×10^6. The lift coefficient range was limited to that where no separation of the air flow across the wing existed, but reached as high as 0.52 with the aid of boundary-layer control.

It was found that at positive angles of attack the vortex sheet assumed a shape which was initially bowed upward but flattened out downstream before the rolling-up process had progressed to an appreciable degree. A comparison with theory showed that an acceptable approximation to the downwash distribution within the distance surveyed could be obtained if the vortex sheet were assumed to be flat and the spanwise vorticity distribution were assumed to be that of the wing.

INTRODUCTION

A considerable number of investigations, both theoretical and experimental, have been undertaken to study the downwash behind wings having straight trailing edges and several theories have been advanced for predicting the downwash behind such wings. However, very little information is available on the downwash behind highly swept-back wings although some methods of calculation have been proposed.

One of the methods of predicting downwash angles behind swept-back wings (reference 1) is an extension of the theory of reference 2 used in predicting the downwash behind high-aspect-ratio straight wings. This theory is based on the assumptions that the trailing vortex sheet extends from the wing trailing edge to infinity in the form of a flat sheet and that the distribution of vorticity across the vortex sheet at any downstream distance remains the same as that on the wing. These same basic assumptions are also made in the flat-sheet methods discussed in parts of references 3 and 4.

The results of reference 1 indicate that these assumptions are valid for use in predicting the downwash angles at several chord lengths behind wings with moderate amounts of sweepback. The characteristics of the flow field behind the highly swept-back wing, however, have not been sufficiently defined experimentally to determine when the assumptions of the flat vortex sheet and undistended vorticity distribution may be applied.

In reference 3 it is stated that behind certain wings of low aspect ratio, the vortex sheet may become essentially rolled up into two trailing vortices within a chord length or less of the wing trailing edge. For this condition the downwash at the tail may be predicted by the use of the rolled-up sheet theory. In this theory the vortex sheet is assumed to be completely rolled up into two vortices at some distance ahead of the point at which the downwash is to be determined. Since reference 3 presents this theory primarily for low-aspect-ratio wings with unswept trailing edges, it is not clear when conditions permit its use for predicting the downwash near the tail location behind a wing with swept-back trailing edges.

It is evident that important factors in the theoretical determination of downwash are the vortex-sheet shape and location and the strength of the tip vortices. To determine these factors and to provide information on the general flow pattern behind a highly swept-back low-aspect-ratio wing, detailed surveys have been made through an extensive region behind a 63° swept-back wing (of aspect ratio 3.5) with fuselage in the Ames 40- by 80-foot wind tunnel. It is the purpose of this report to make available these data, to point out some of the more important features, and to determine if the downwash from the subject wing can be approximated by existing theories.

Presented in this report are downwash contour maps for longitudinal stations located between 0.57 semispan and 2.71 semispans aft of the 0.25 mean aerodynamic chord point. Figures showing the variations of the shape of the vortex sheet at the various longitudinal stations are also presented. A brief comparison of the flat sheet and rolled-up sheet concepts of theoretically predicting downwash is also presented.

SYMBOLS

b   wing span, feet

c   section chord of wing, measured parallel to the plane of
        symmetry, feet

c_{av} average chord of wing, feet

$\bar{c}$ mean aerodynamic chord $\left(\dfrac{\int_0^{b/2} c^2 dy}{\int_0^{b/2} c\ dy} \right)$, feet

C_L wing lift coefficient $\left(\dfrac{lift}{qS} \right)$

c_l section lift coefficient

q   free-stream dynamic pressure, pounds per square foot

S   wing area, square feet

x   distance in free-stream direction measured from the 0.25 mean
        aerodynamic chord point of the wing, feet

y   spanwise distance from the plane of symmetry, feet

z   vertical distance measured from the wing chord plane extended,
        feet

α angle of attack of wing corrected for tunnel-wall effect and
        flow inclination, degrees

α_{corr} angle of attack, corrected for change in α due to the survey
        apparatus, degrees

ϵ downwash angle, measured relative to the free-stream direction,
        degrees

ϵ_{max} maximum downwash angle for each angle of attack at given x and y
        positions behind the wing, degrees

DESCRIPTION OF MODEL AND APPARATUS

The geometric characteristics of the model are shown in figure 1. The wing had 63° sweepback of the leading edge, an aspect ratio of 3.5, and a taper ratio of 0.25. There was 0° twist, dihedral, and incidence. The wing had a 64A006 section parallel to the plane of symmetry.

The fuselage had a fineness ratio of 11.4 based on the actual fuselage length. The cross section of the fuselage was circular except where the blower exhaust duct projected from the lower part of the fuselage. A photograph of the model mounted in the tunnel is shown in figure 2.

In order to obtain downwash angles of suitable magnitude without changes in span loading due to separation on the wing, the wing leading edge was equipped with area suction as a boundary-layer-control device which in this case prevented separation at lift coefficients slightly above 0.52.

The survey apparatus, also shown in figure 2, was suspended from longitudinal rails fixed to the top of and extending the length of the test section of the tunnel. Transverse rails mounted on the main carriage permitted lateral movements across the survey area. Major changes in the vertical displacement of the survey rake were made by rotating the rake support nacelle about the longitudinal axis of the control cab. Minor changes were made by rotating the rake support boom about the longitudinal axis of the support nacelle.

The survey rake consisted of six tubes of the combined pitch, yaw, and dynamic-pressure type mounted on the support boom in two vertical rows of three tubes each. The tubes were spaced 18 inches apart both vertically and horizontally.

TESTS

The survey was conducted at an airspeed of approximately 78 miles per hour which resulted in a Reynolds number, at standard atmospheric conditions, of 6.1×10^6 based on the mean aerodynamic chord.

Surveys were made at three angles of attack, 4.1°, 8.2°, and 12.3°, with downwash and dynamic-pressure data being obtained in nine vertical transverse planes located between 0.57 and 2.71 semispans aft of the quarter-chord point of the mean aerodynamic chord (fig. 3). The angles of attack investigated did not exceed 12.3° since at higher angles the air flow across the wing tips became slightly unstable even though the

wing tips did not actually stall until an angle of attack of 14.4° was
reached.

In the survey planes aft of the plane of the wing-tip trailing edge,
the survey extended spanwise from the plane of symmetry to 1.2 semispans
in order to determine the spanwise location of the center of the vortex
core as well as the location of the vortex sheet. The limits of the
vertical heights of the survey varied according to the limits of the
survey apparatus or to the heights at which the magnitude of the down-
wash angles was essentially 0°. The lateral spacing of the data points
are given in the following table:

Spanwise location, semispans	Lateral spacing (in.)
0 to 0.55	18.0
.55 to .78	9.0
.78 to 1.00	4.5
1.00 to 1.20	9.0

All vertical spacings were 4.5 inches. There were approximately 400 data
points for each survey plane, with the exception of the survey planes in
the region between the wing trailing edge and fuselage. There the data
points were omitted where there was interference between the survey
apparatus and the model.

In order to correlate the downwash data with lift coefficient, lift-
force data were obtained through the angle-of-attack range of the test
with the survey apparatus being located at each of the longitudinal sta-
tions surveyed (fig. 4).

CORRECTIONS

The measured downwash angles and angles of attack were corrected
for tunnel air-stream inclination and the air-stream inclination due
to the presence of the survey apparatus. The latter correction was
obtained from tare runs made with the model at the angle of attack for
zero lift with the survey apparatus at each survey position. This tare
includes the thickness effect of the wing and fuselage.

Tunnel-wall corrections applied to the downwash angles and angles
of attack were determined theoretically by the image system method for a

swept-back wing in a rectangular tunnel. After computing the correction coefficients for the 2.36 b/2 and 2.71 b/2 longitudinal stations, it was found that these coefficients differed by less than 10 percent from the correction coefficients for a straight wing of the same span and area. This magnitude of differences was considered to be negligible, therefore the correction coefficients of the straight wing were applied throughout the survey. The angle change to the downwash varied with longitudinal distance aft of the wing

from $\Delta\epsilon = 0.192\ C_L$

to $\Delta\epsilon = 0.535\ C_L$

and the angle of attack was corrected by

$$\Delta\alpha = 0.482\ C_L$$

Corrections were not applied to the wake displacement since the effects of the tunnel wall and the effects of the survey apparatus were small and opposite in sign so that the resultant change in wake displacement was considered negligible.

RESULTS AND DISCUSSION

Downwash Data

The downwash data obtained from the investigation are presented as maps of contours of constant downwash angles. The maps represent each of the vertical transverse planes surveyed at each angle of attack (figs. 5, 6, and 7).

The vertical distances are referenced to the extended chord plane for each angle of attack with the longitudinal distances being measured horizontally from the quarter-chord point of the mean aerodynamic chord.

In the form presented, the data are of primary interest as a basis for judging the accuracy of the predictions of a downwash theory or for use in the design of an airplane having a similar configuration. However, in so using these data, consideration should be given to the distortion introduced into the downwash field by the effects of the support struts. This influence can be seen in the vicinity of the 0.40 semispan station.

Shape and Location of the Vortex Sheet

Important factors in downwash theory, which are not obtainable from downwash-angle measurements alone, are the shape and location of the vortex sheet. These factors can, however, be determined from a study of the maximum momentum loss in the wake which is very nearly coincident with the vortex sheet. Momentum-loss data taken during this investigation have been analyzed for the purpose of defining the vortex-sheet shape and location.

Figure 8 shows the result of this analysis in the form of the spanwise variation of the vortex-sheet height with respect to the extended chord plane at each angle of attack and survey plane. In the region between the wing trailing edges and for a considerable distance aft of the plane of the wing-tip trailing edges, the vortex sheet is found to be bowed upward, being highest near the wing-fuselage intersection.[1] This apparently results in part from the fact that the trailing edge of a swept-back wing at angles of attack does not lie in a single horiztonal plane. At positive angles of attack, the sweepback of the wing trailing edges causes the trailing edge at the wing tip to lie in a lower horizontal plane than the trailing edge at the plane of symmetry and this shape is assumed to some extent by the free vortex sheet. It must be pointed out, however, that the bowing up of the vortex sheet is not peculiar to wings with swept-back trailing edges. This condition has also been observed to exist behind certain wings with straight trailing edges.

Path of the Vortex Core

Another factor in controlling the pattern of the downwash field is the development of the vortex core. In the case of the unswept wing of higher aspect ratio, the rolling up of the vortex sheet is not sufficiently advanced, within the tail lengths of interest, to affect the downwash appreciably; therefore a flat sheet is assumed. However, in the case of the low-aspect-ratio wing with straight trailing edges, it has been shown (reference 3) that the vortex sheet may roll up into tip vortices within tail lengths of interest. Therefore, a fully rolled-up sheet of two discrete vortices is assumed for this case. The downwash

---

[1]In considering these results, the shape of the vortex sheet inboard of the 0.20 semispan station should be ignored since it is influenced by fuselage interference.

data presented in this report have been analyzed in an attempt to deter-
mine if either of these cases is applicable to a highly swept-back low-
aspect-ratio wing.

Reference 3 shows that the lateral position of the center of gravity
of the vortices trailing from each half of the wing remains invariant
with increasing distance aft of the wing. In the rolling-up process the
vorticity in the sheet is continually being shifted outboard into the tip
vortex. Thus, as the tip vortex gains strength it must move inboard in
order to maintain the center-of-gravity position. Hence, the amount of
inboard displacement of the tip vortex at any downstream station indicates,
at least qualitatively, the amount of rolling up that has taken place
ahead of that station.

The location of the tip vortex at each longitudinal station is
easily discernible in the downwash contours (figs. 5, 6, and 7) as a
concentration of contour lines near the 1.00 semispan station. Here it
may be seen that there is a slight lateral displacement at the survey
plane nearest the wing-tip trailing edge but that there is little dis-
placement from that point to the aftermost survey plane. Reference 5
also shows this same type of vortex-core path behind a 35° swept-back
wing.

Figure 9 compares the tip vortex path obtained experimentally with
that computed from the theory in reference 3. This theory considers the
origin of the coordinate system of the tip vortex to lie at the edge of
the unrolled vortex sheet and that the y axis of the coordinate system
is tangent to the flat portion of the sheet. Therefore, in order to
keep the theory compatible with the experimental results, the y and z
axes of the theory were rotated so that the y axis was tangent to the
flat portion of the experimental bowed-up sheet. The spanwise location
of the completely rolled-up vortex was computed to be 0.853 semispan,
with the path of the vortex being displaced approximately 70 percent of
this amount at the 2.71 longitudinal station. This predicted amount of
displacement indicates that a considerable amount of the rolling-up
process should have been completed ahead of the 2.71 semispan longitudinal
station. At this point, however, the experimental data show that the
tip vortex has been displaced only 10 percent of the amount required for
complete roll up, thus indicating that very little of the rolling-up
process has been completed. Since this experimental lateral displacement
is less than the amount which was considered to be negligible in refer-
ence 2, the effect of the tip vortices on the downwash field, within the
limits of this survey, may be neglected as in reference 2.

Comparison of Theories With Experimental Results

Lacking a generalized downwash theory, comparison of the downwash can be made only with theoretical values representing the limiting assumptions of either no roll up of the vortex sheet or complete roll up into the tip vortices. Of the several analytical procedures possible, the method of reference 4 was used because of its simplicity. Where the experimental span loading is used, the downwash corresponding to a flat vortex sheet is obtained; where uniform loading is used, the method gives the downwash obtained when the vortex sheet is completely rolled up into the two tip vortices. The span loading curves used in the computations are shown in figure 10.

In order to determine which method yields the more accurate prediction of the downwash angles at the various lateral positions, comparison is made of the distribution of ϵ_{max} in the spanwise direction at two angles of attack and two distances downstream from the wing. No attempt has been made to compare the vertical locations of ϵ_{max} given by the predictions with those found experimentally.

The experimental data of figures 5, 6, and 7 were cross-plotted to obtain the downwash angles which would result if the corrected angles of attack of the model were constant throughout the longitudinal positions surveyed. In figure 11, a comparison of these results with the two theories indicates that the flat-sheet concept approximates the downwash distribution quite closely at both longitudinal distances at $\alpha = 6.0^{\circ}$, and at the 2.71 b/2 longitudinal point at $\alpha = 10.5^{\circ}$. At the 1.31 b/2 longitudinal point at $\alpha = 10.5^{\circ}$, even though the magnitude of the predicted downwash angles is higher than that of the experimental downwash angles, the general distributions are in agreement.

From the above results, it is seen that the theory assuming the flat vortex sheet will closely approximate the downwash distribution when used with the experimental span loading provided there is no separation of the air flow across the wing.

CONCLUSIONS

The investigation of the downwash characteristics and vortex-sheet shape behind a 63° swept-back wing-fuselage combination indicated the following:

1. At positive angles of attack the vortex sheet was bowed upward in the region near the wing. This was attributed partly to the sweepback of the wing trailing edge.

2.   The rolling up of the vortex sheet proceeded in such a manner
that the theory assuming a flat vortex sheet gave acceptable predictions
of the downwash distributions within the limits of this survey.

Ames Aeronautical. Laboratory
     National Advisory Committee for Aeronautics
          Moffett Field, Calif.

REFERENCES

1. Furlong, G. Chester, and Bollech, Thomas V.:   Downwash, Sidewash,
      and Wake Surveys Behind a 42° Sweptback Wing at a Reynolds Number
      of 6.8×10^6 With and Without a Simulated Ground.
      NACA RM L8G22, 1948.

2. Silverstein, Abe, Katzoff, S., and Bullivant, W. Kenneth: Downwash
      and Wake Behind Plain and Flapped Airfoils.   NACA Rep. 651, 1939.

3. Spreiter, John R., and Sacks, Alvin H.:   The Rolling Up of the
      Trailing Vortex Sheet and Its Effect on the Downwash Behind Wings.
      Jour. Aero. Sci., vol. 18, no. 1, Jan. 1951, pp. 21-32.

4. DeYoung, John: Theoretical Symmetric Span Loading Due to Flap
      Deflection for Wings of Arbitrary Plan Form at Subsonic Speeds.
      NACA TN 2278, 1951.

5. Luetgebrune, H.:   Nachlauf- und Widerstandsuntersuchungen an
      gepfeilten und ungepfeilten Tragflugeln.   Zentrale für
      Wissenschaftliches Berichtwesen der Luftfahrtforschung, FB 1672,
      Berlin, Sept. 20, 1942.
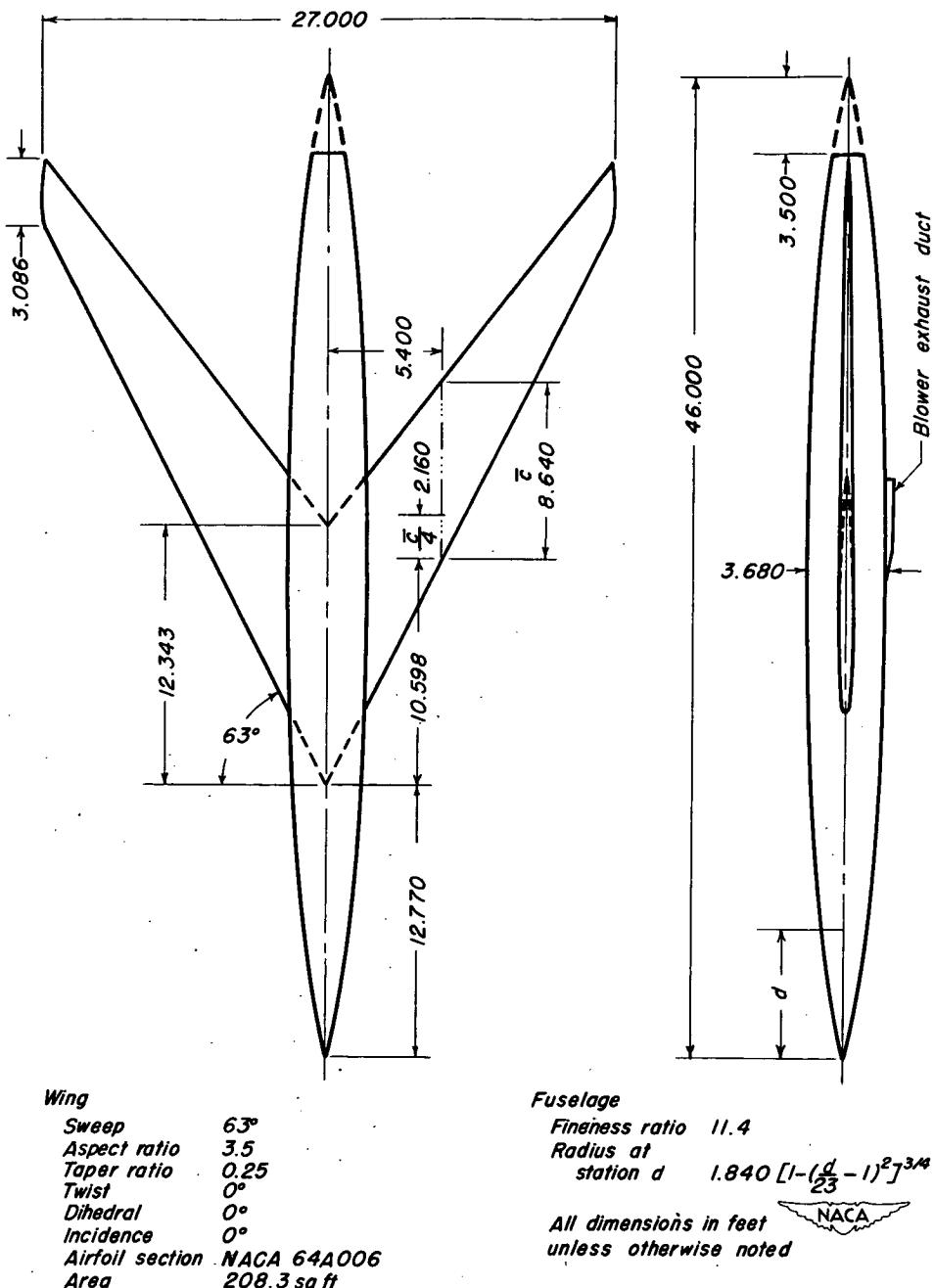
Figure 1.- Geometric characteristics of the 63° swept-back wing-
fuselage combination.
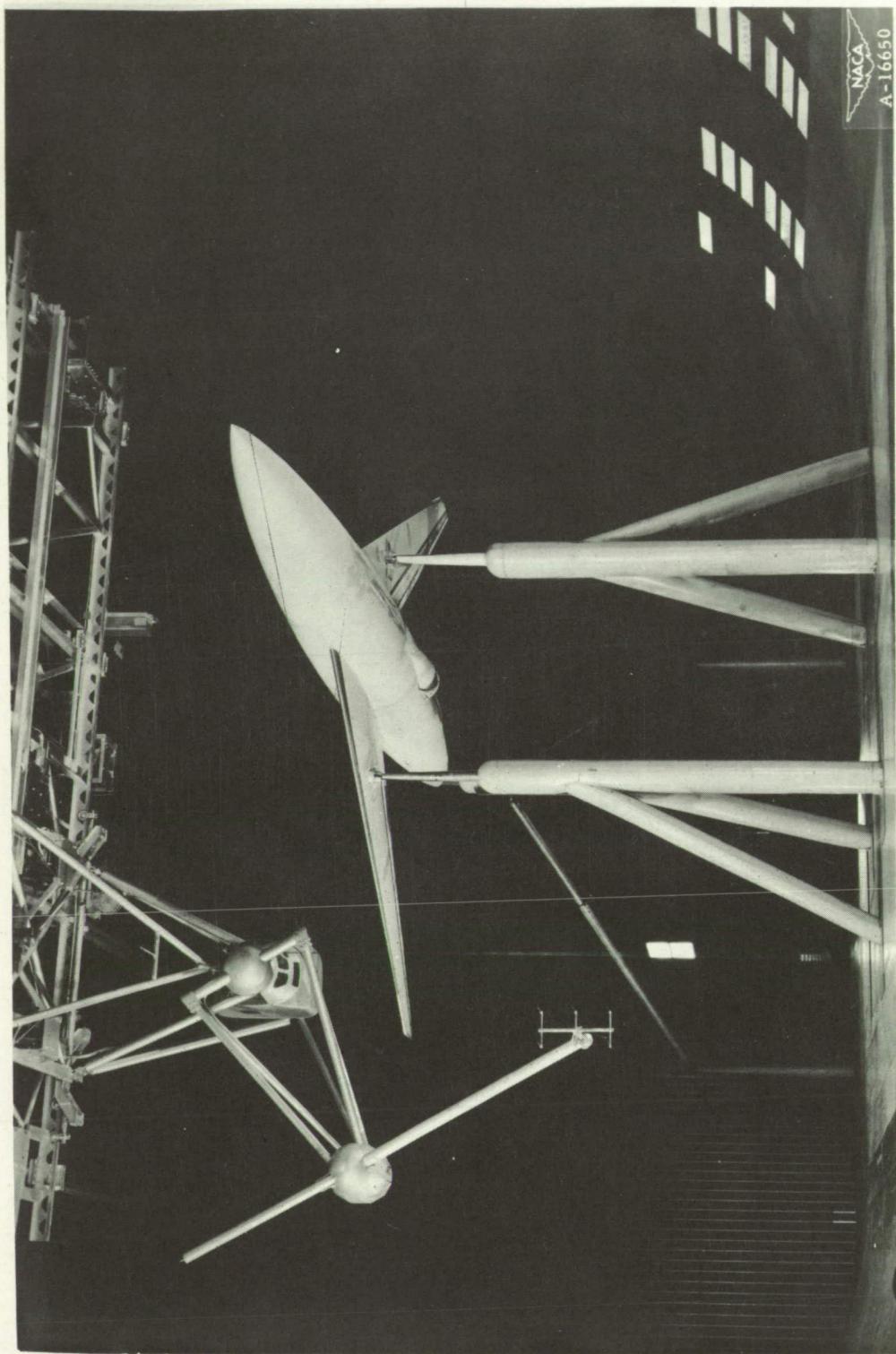
Figure 2.— The 63° swept-back wing—fuselage combination mounted in the Ames 40— by 80—foot wind tunnel with the survey apparatus behind the wing.
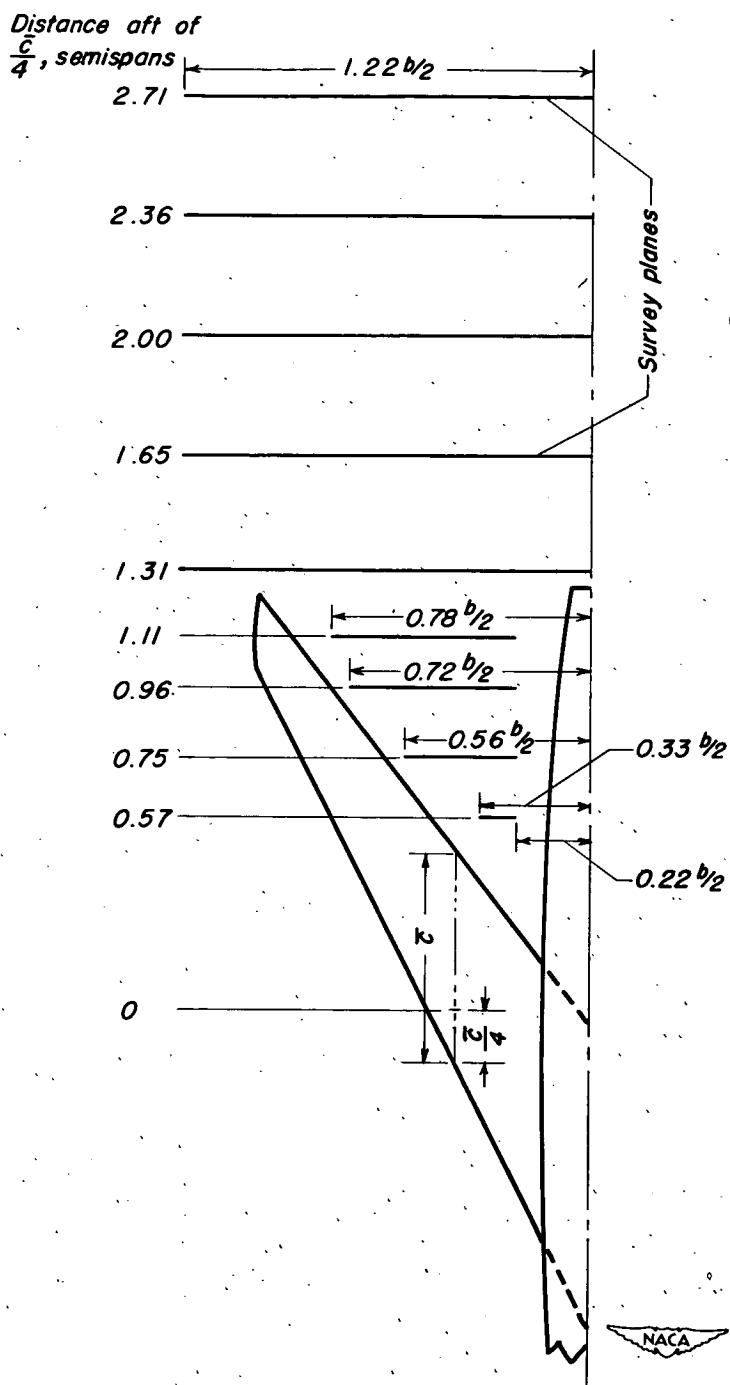
Figure 3 .— Location of downwash survey planes behind the 63°
swept-back wing-fuselage combination.
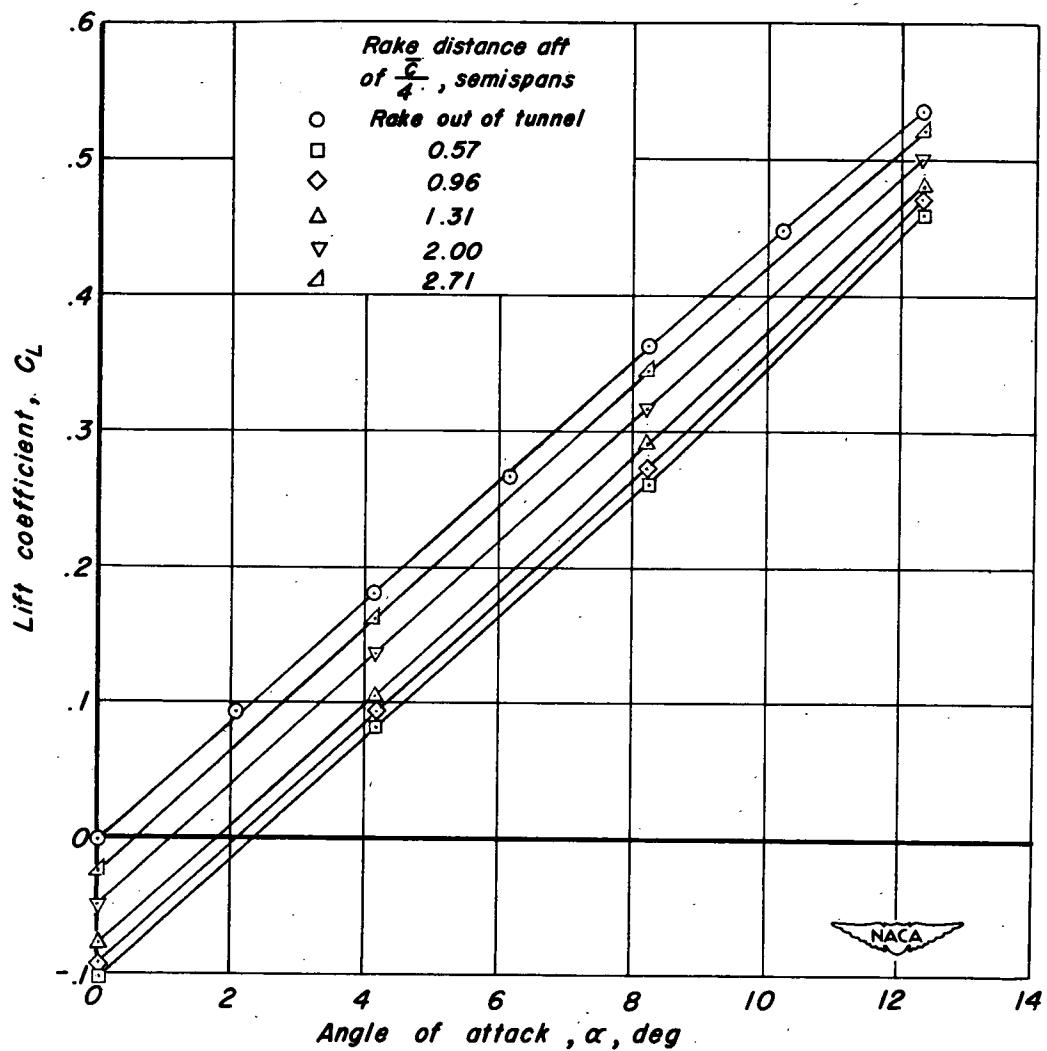
Figure 4.— Variation of lift coefficient with angle of attack for various longitudinal positions of the survey rake. Angle of attack corrected for tunnel–wall effect and flow inclination.

(b) x = 0.75 b/2, a_{corr} = 2.0°

(a) x = 0.57 b/2, a_{corr} = 1.9°
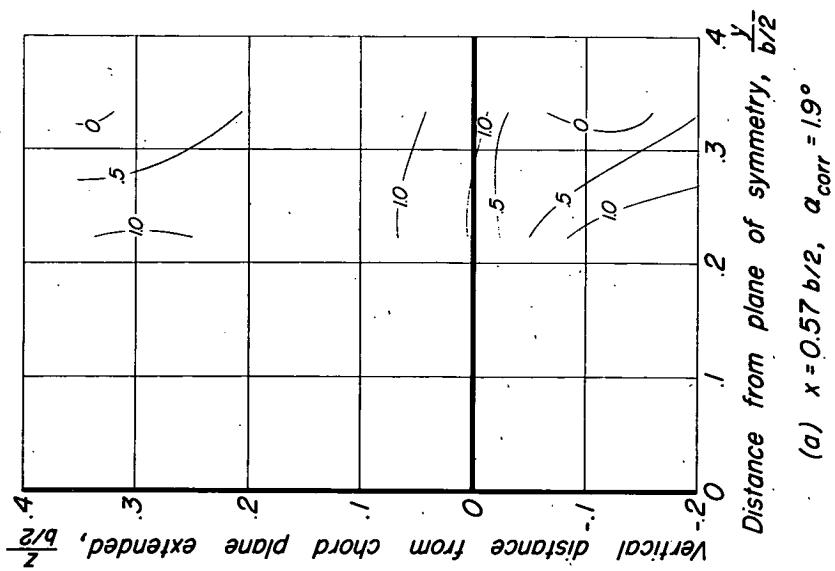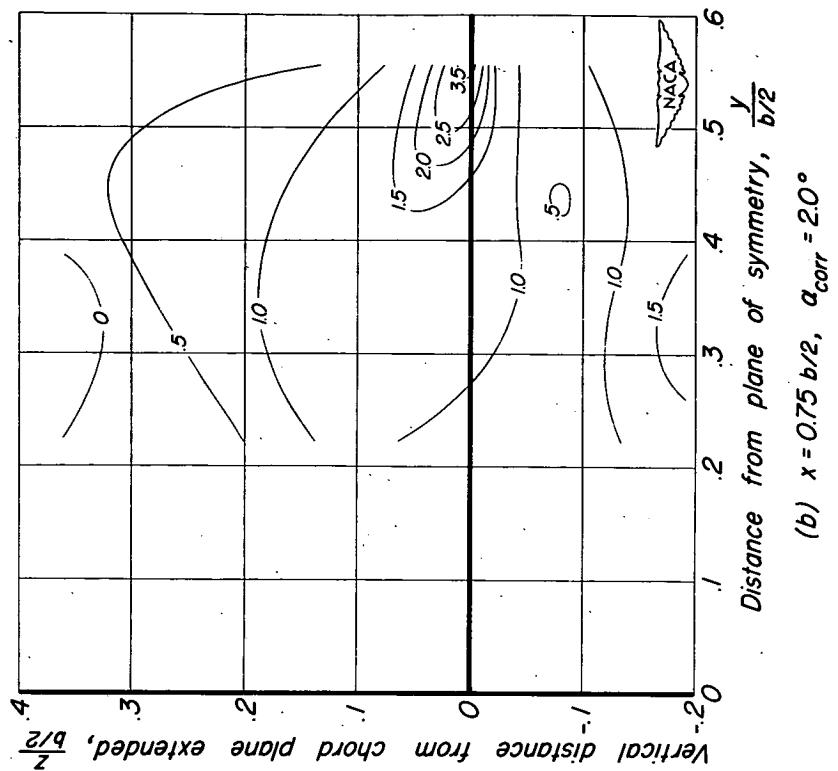
Figure 5.— Contours of constant downwash angles in vertical planes normal to the plane of symmetry behind the 63° swept-back wing-fuselage combination. α = 4.1°.
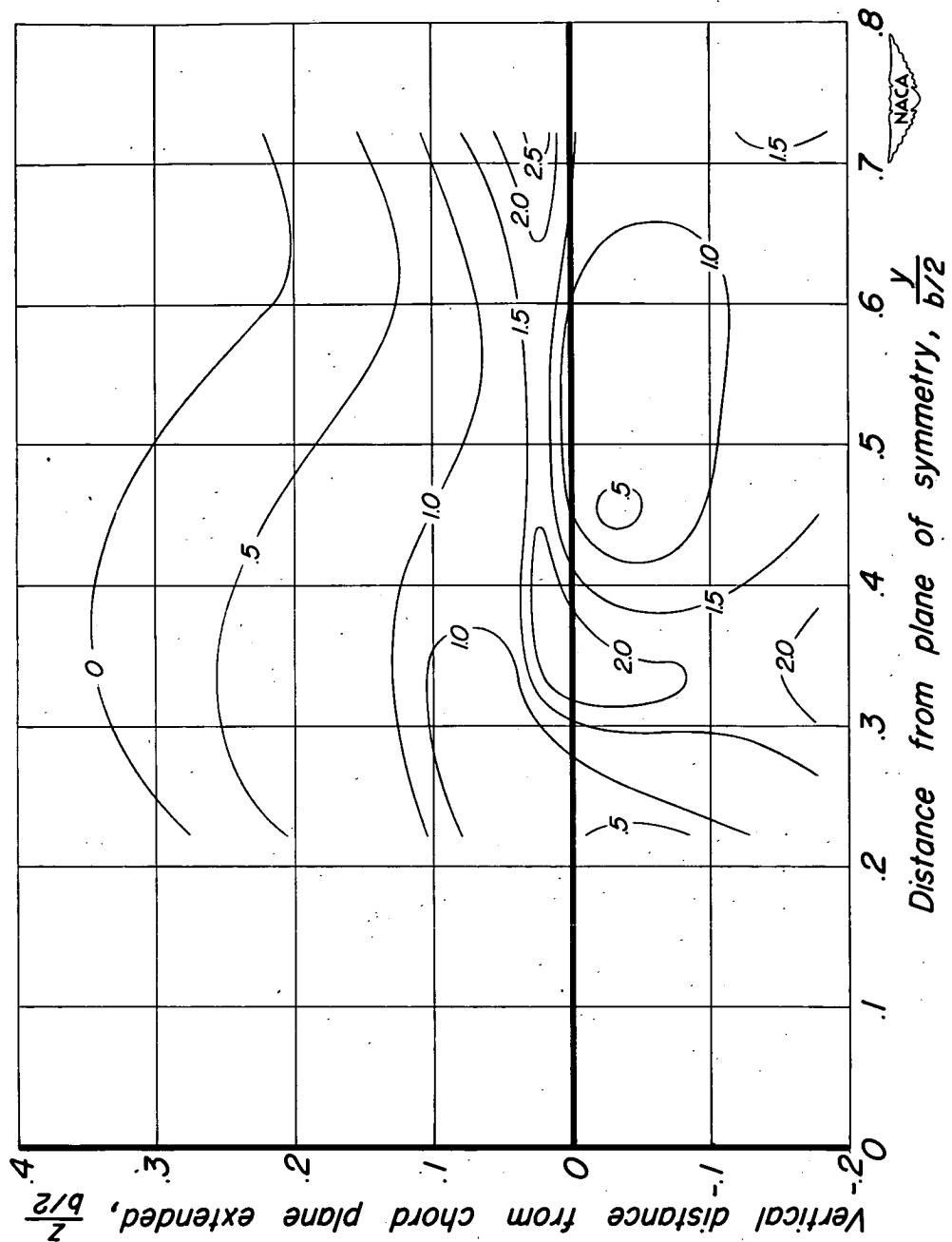
(c) $x = 0.96 \, b/2$, $\alpha_{corr} = 2.2°$

Figure 5.— Continued.
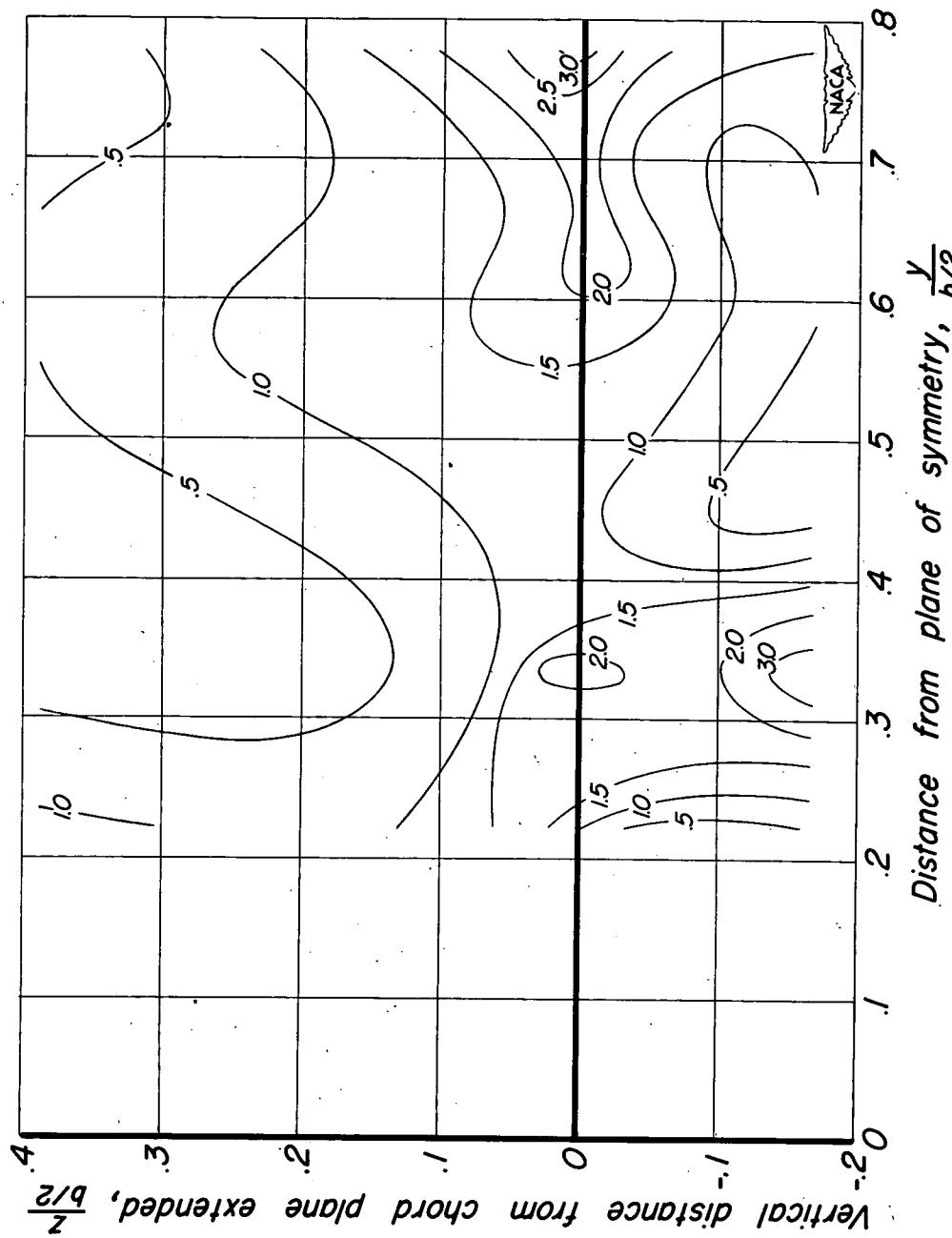
(d) $x = 1.11 \ b/2$, $\alpha_{corr} = 2.3°$

Figure 5.— Continued.

(e) $x = 1.31$ $b/2$, $a_{corr} = 2.4°$
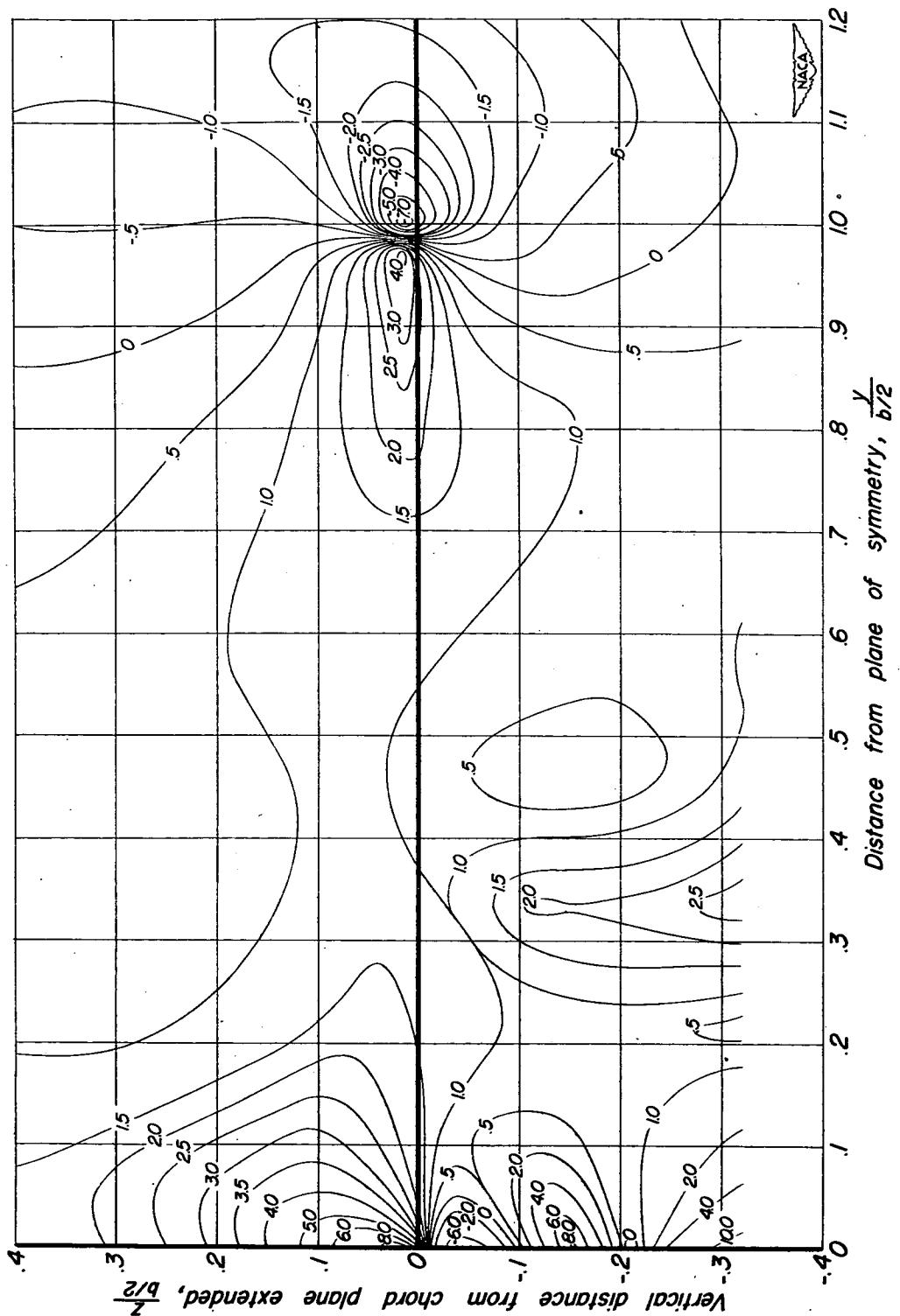
Figure 5.— Continued.
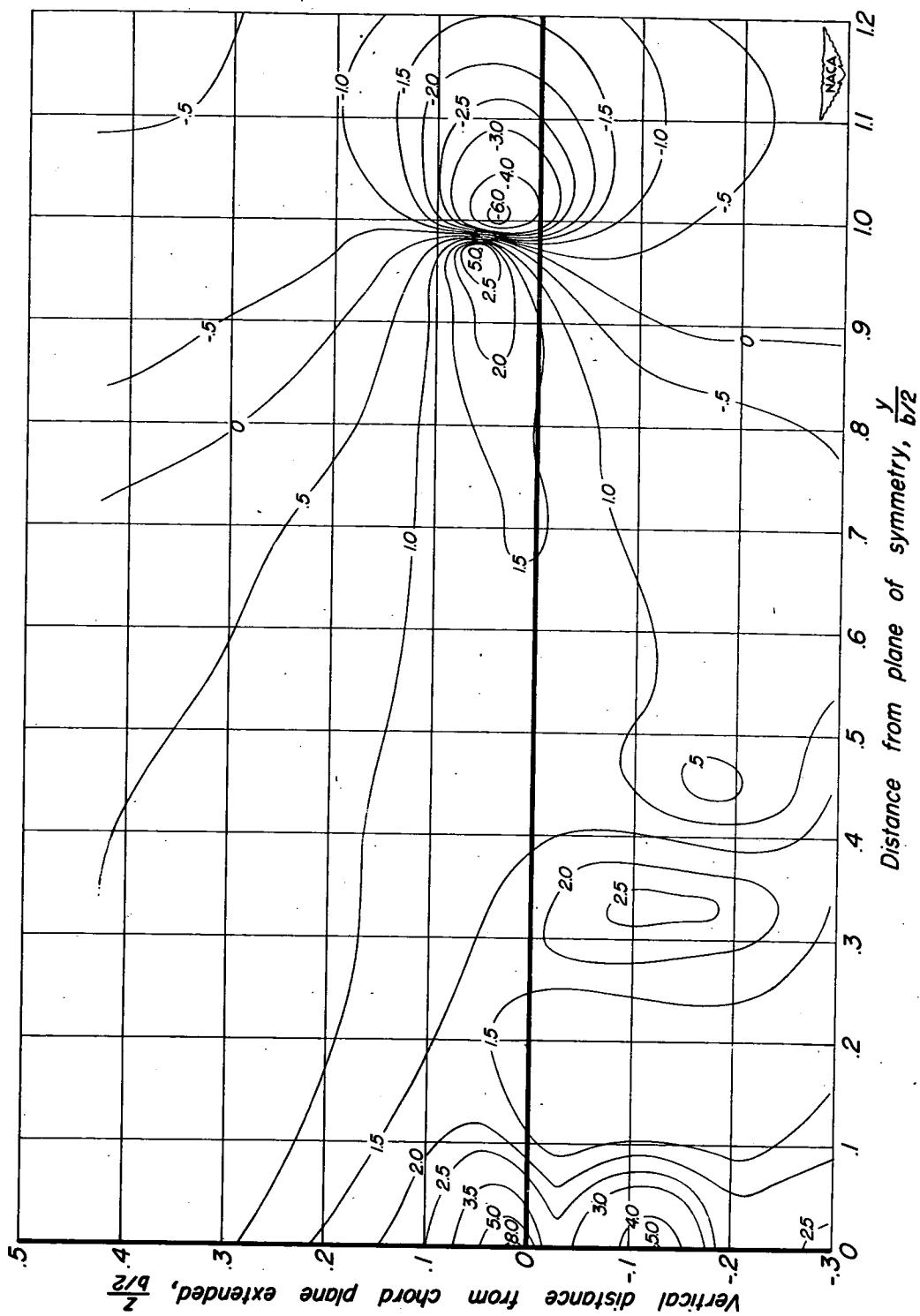
(f) x = 1.65 b/2, a_corr = 2.8°

Figure 5.—Continued.

(g) $x = 2.00\ b/2$, $a_{corr} = 3.1°$
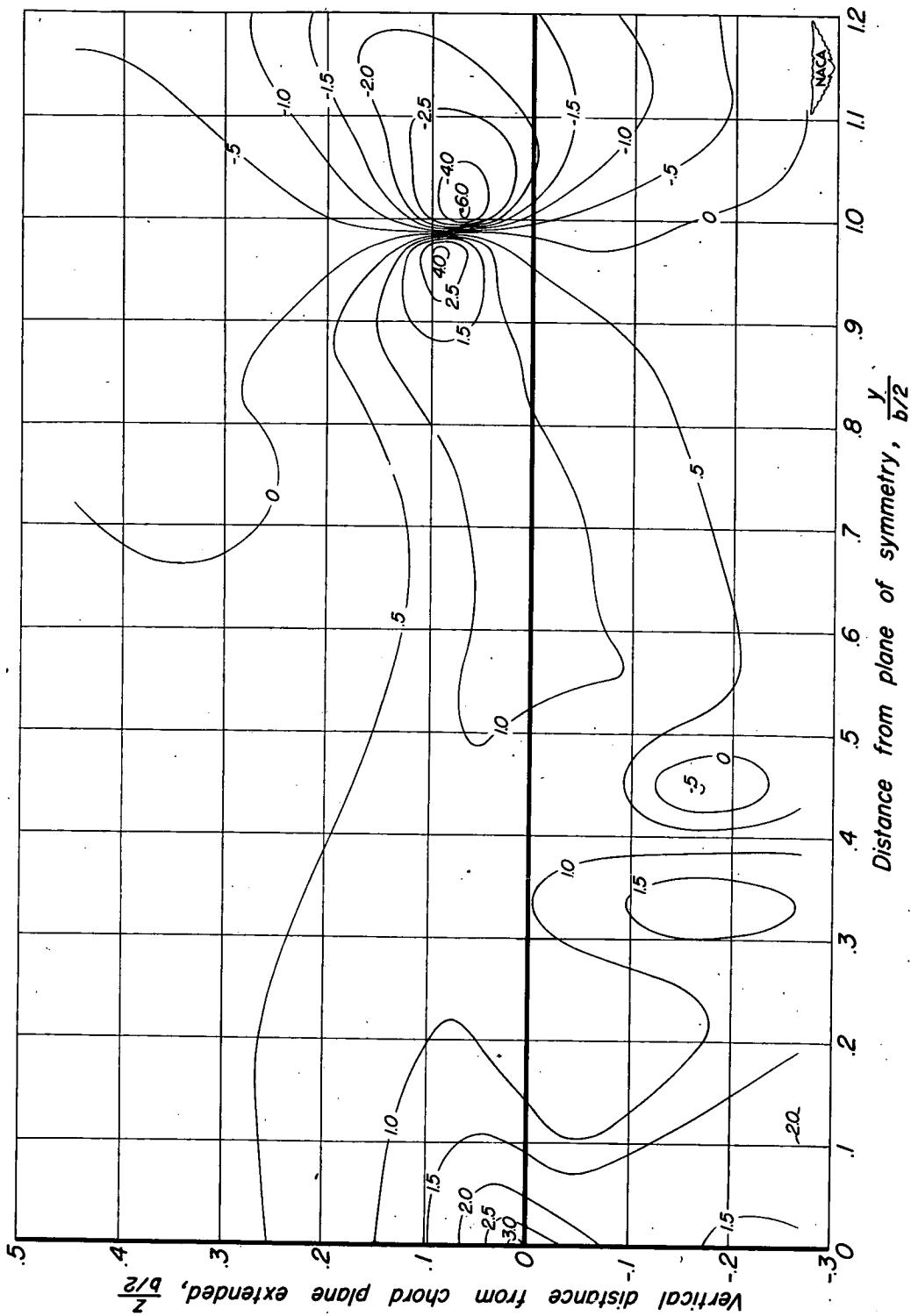
Figure 5.—Continued.

(h) x = 2.36 b/2, a_{corr} = 3.4°

Distance from plane of symmetry, $\frac{y}{b/2}$

Vertical distance from chord plane extended, $\frac{z}{b/2}$

Figure 5.— Continued.

Distance from plane of symmetry, $\frac{y}{b/2}$

(i) x = 2.71 b/2, a_{corr} = 3.7°
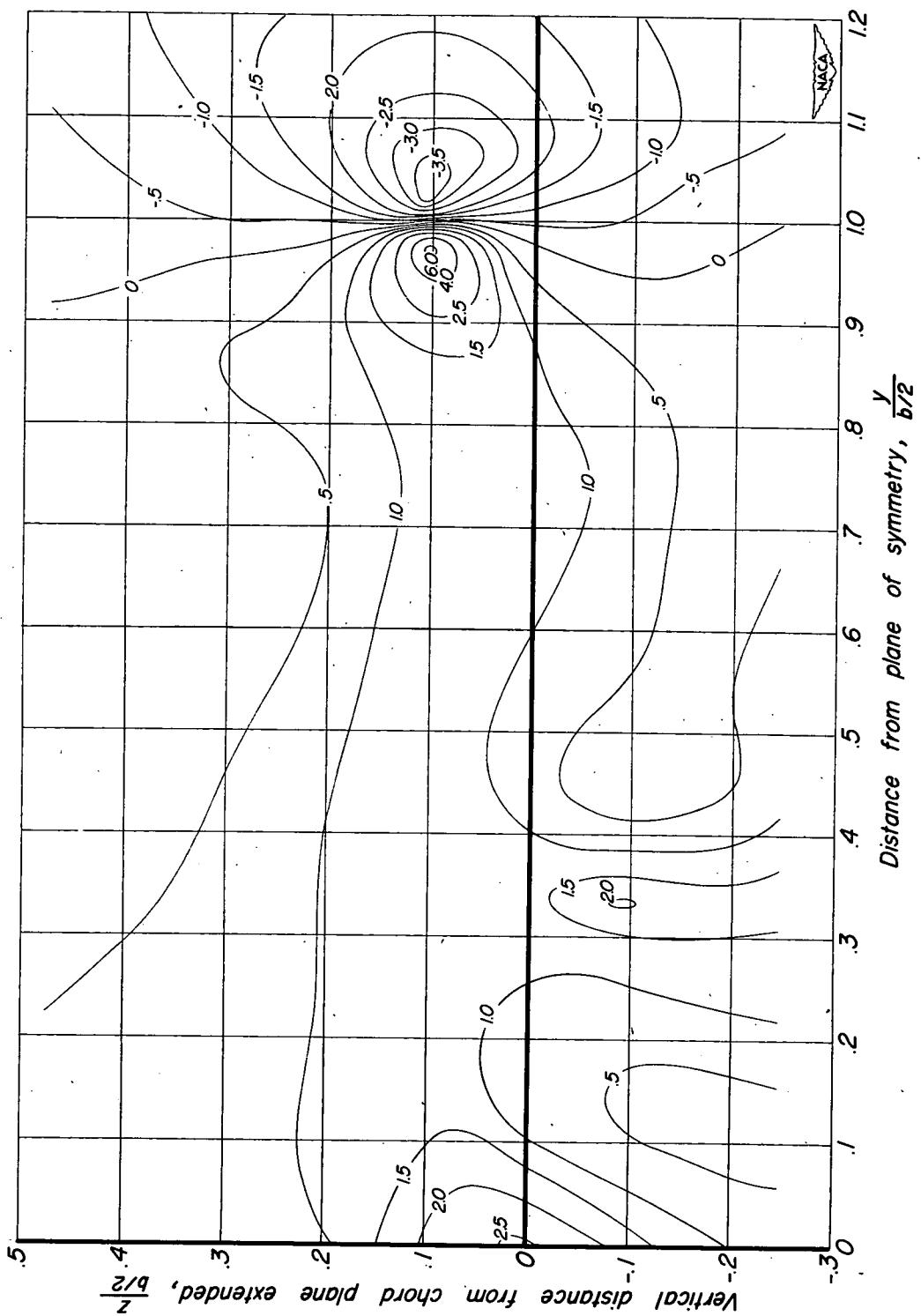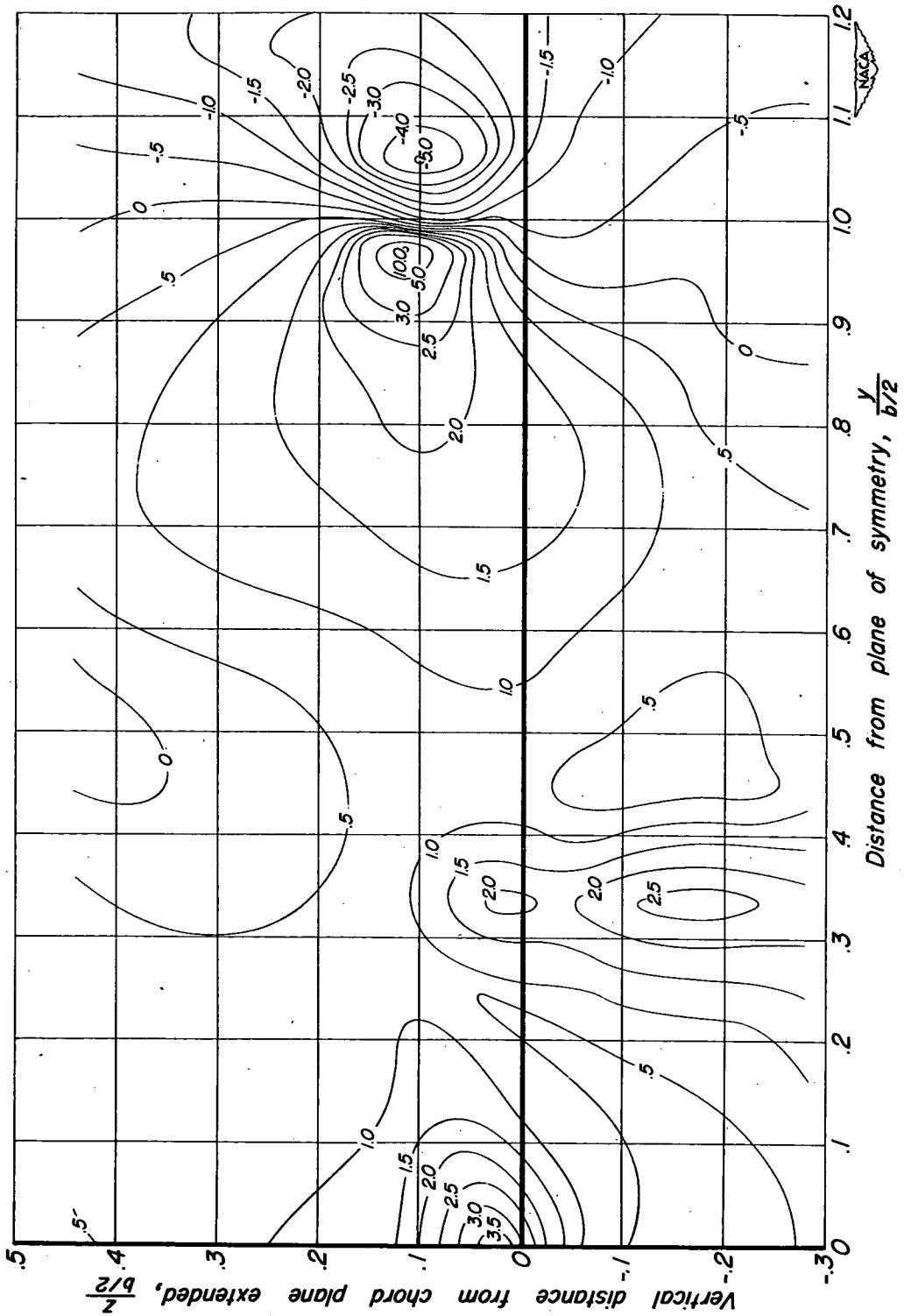
Figure 5.—Concluded.
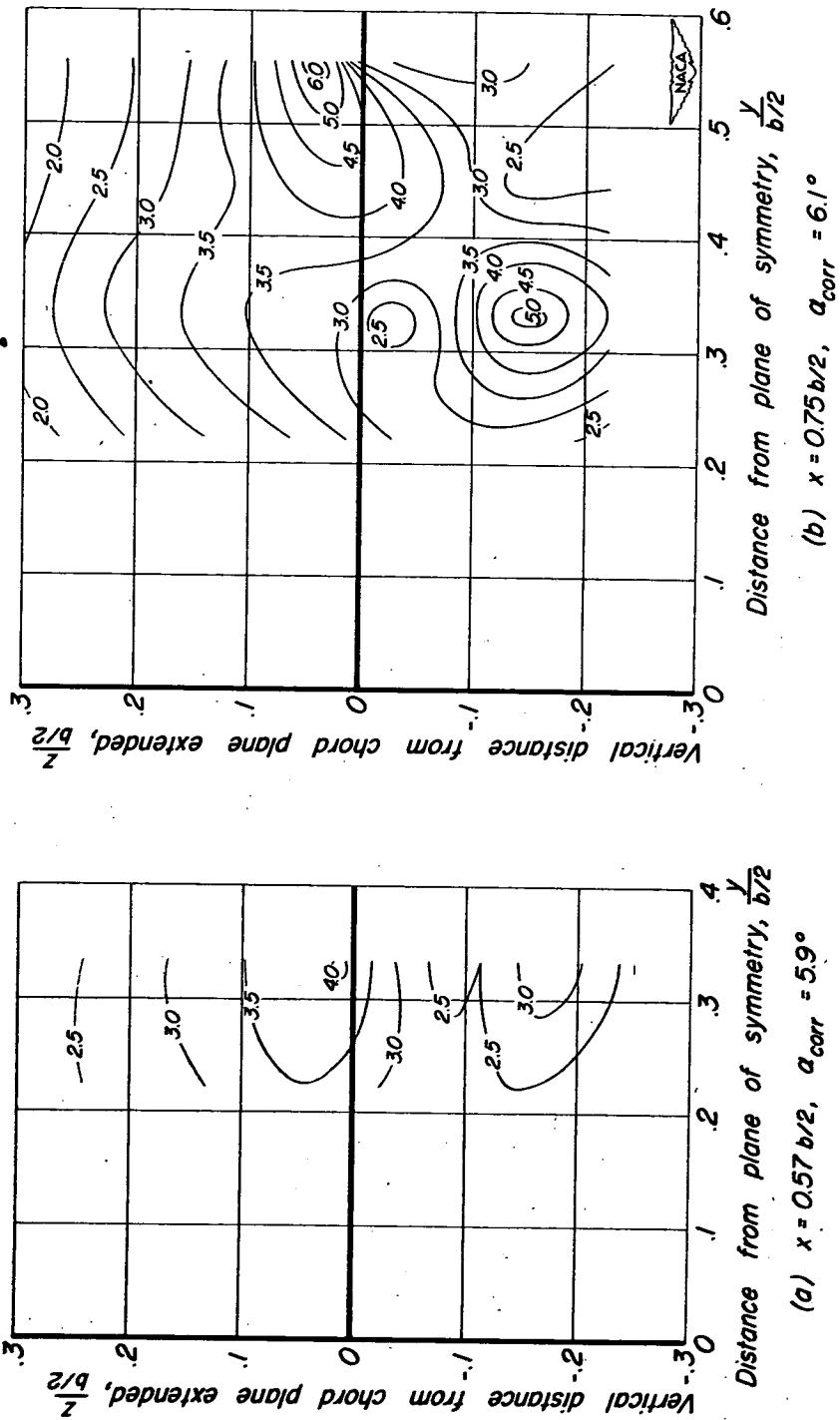
Figure 6.— Contours of constant downwash angles in vertical planes normal to the plane of symmetry behind the 63° swept-back wing-fuselage combination. $\alpha = 8.2°$.

Distance from plane of symmetry, $\frac{y}{b/2}$
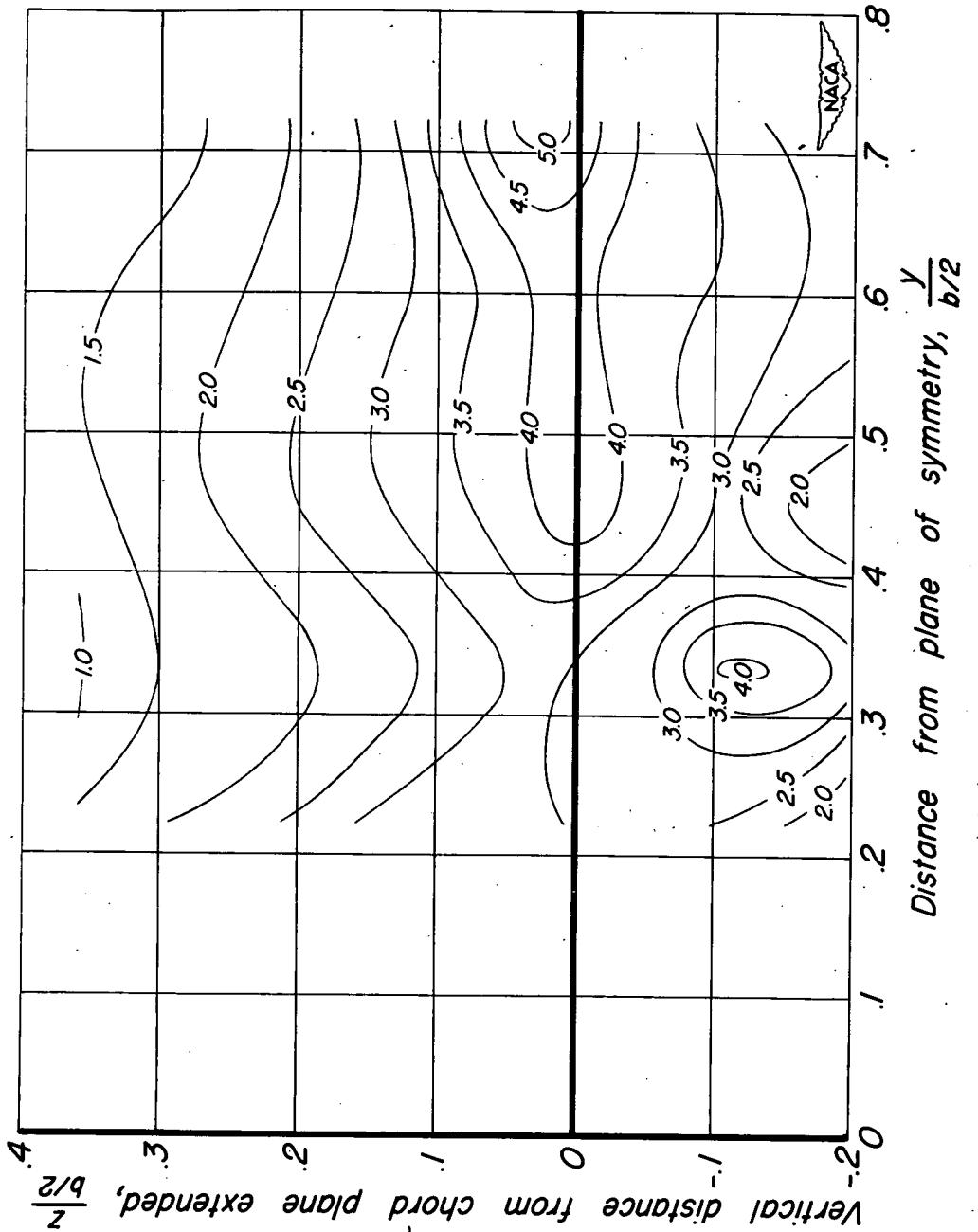
(c) x = 0.96 b/2, α_{corr} = 6.2°

Figure 6.— Continued.
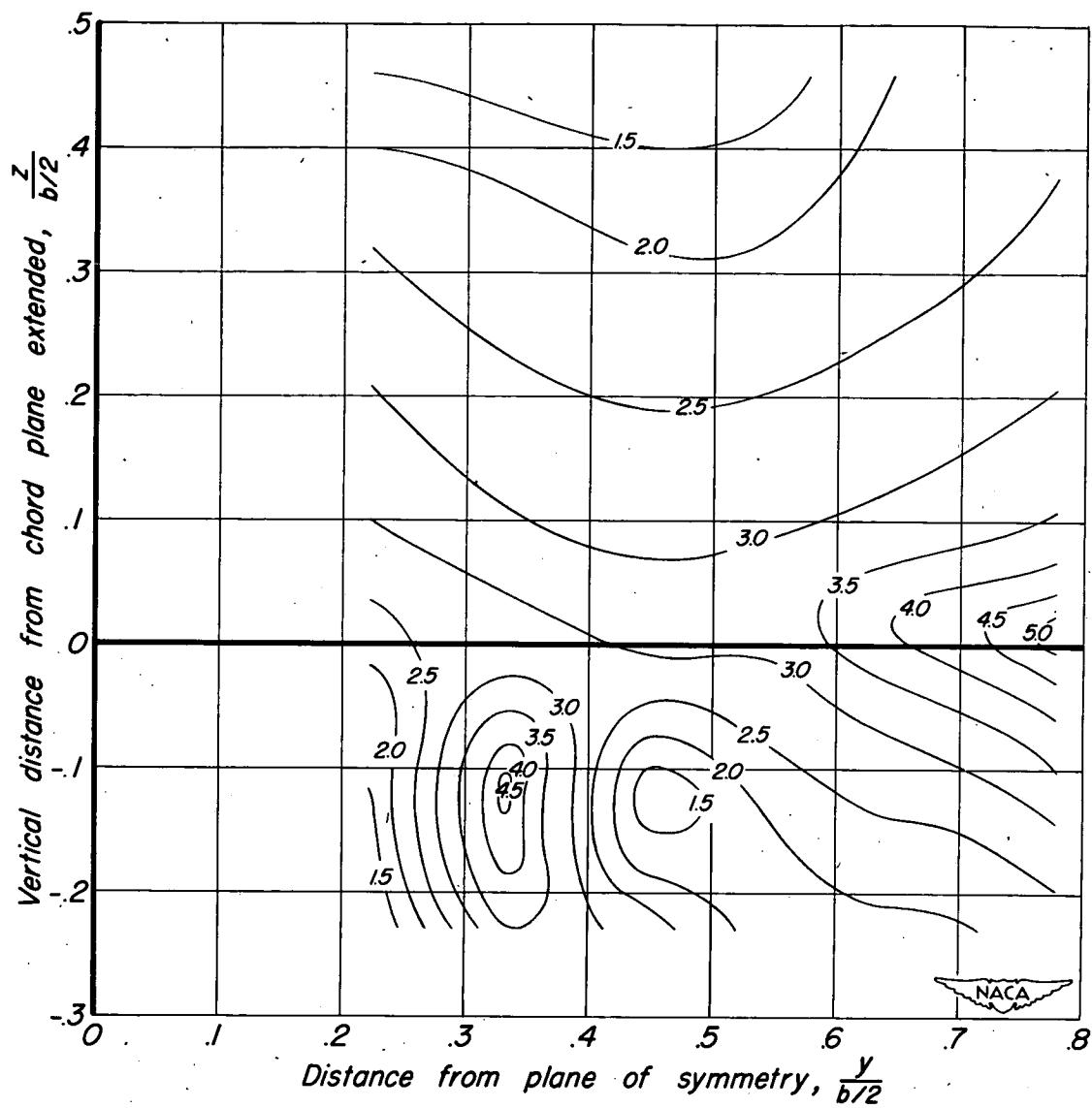
(d) x = 1.11 b/2, α_{corr} = 6.4°

Figure 6.— Continued.
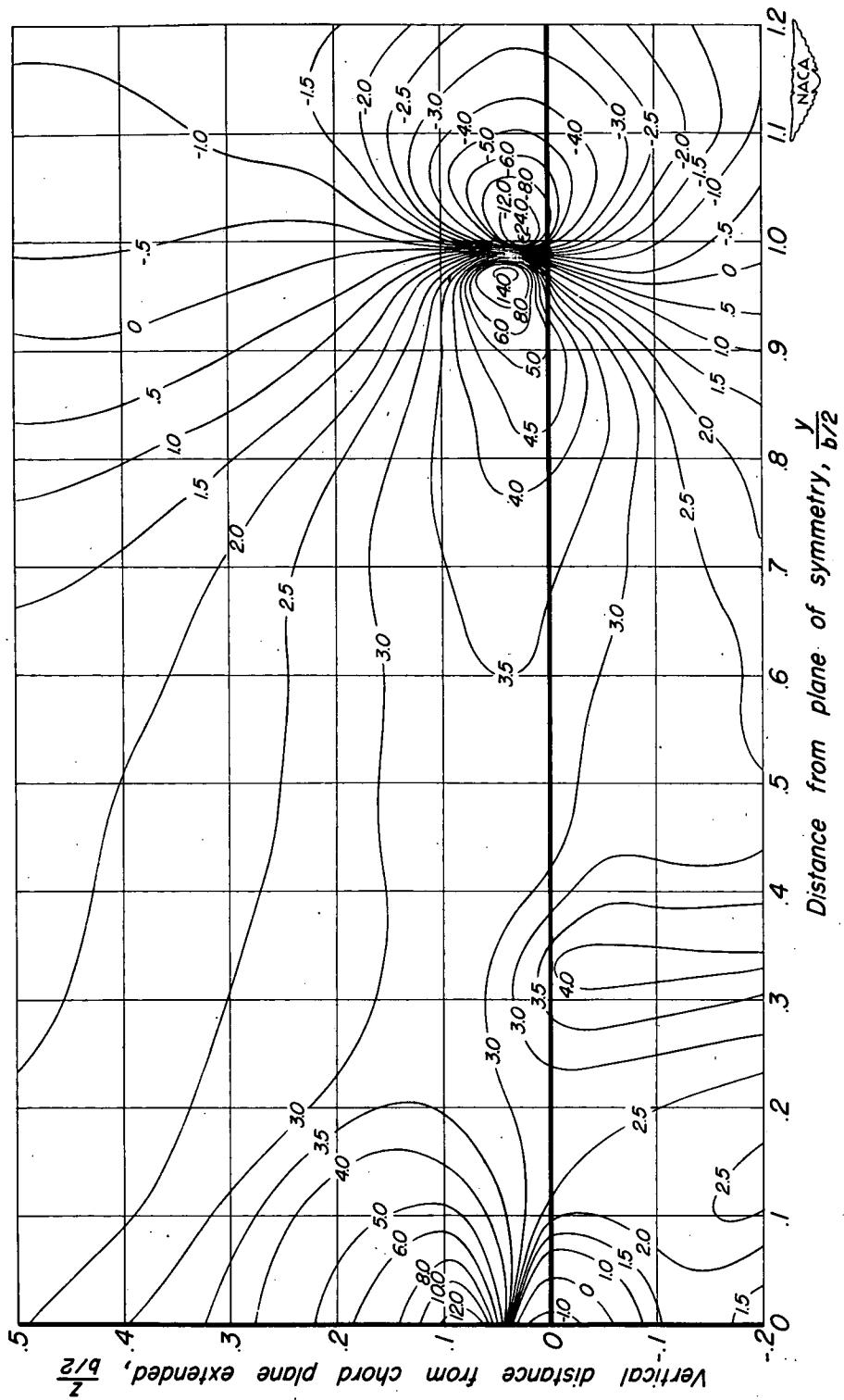
(e) x = 1.31 b/2, a_corr = 6.6°

Figure 6.— Continued.
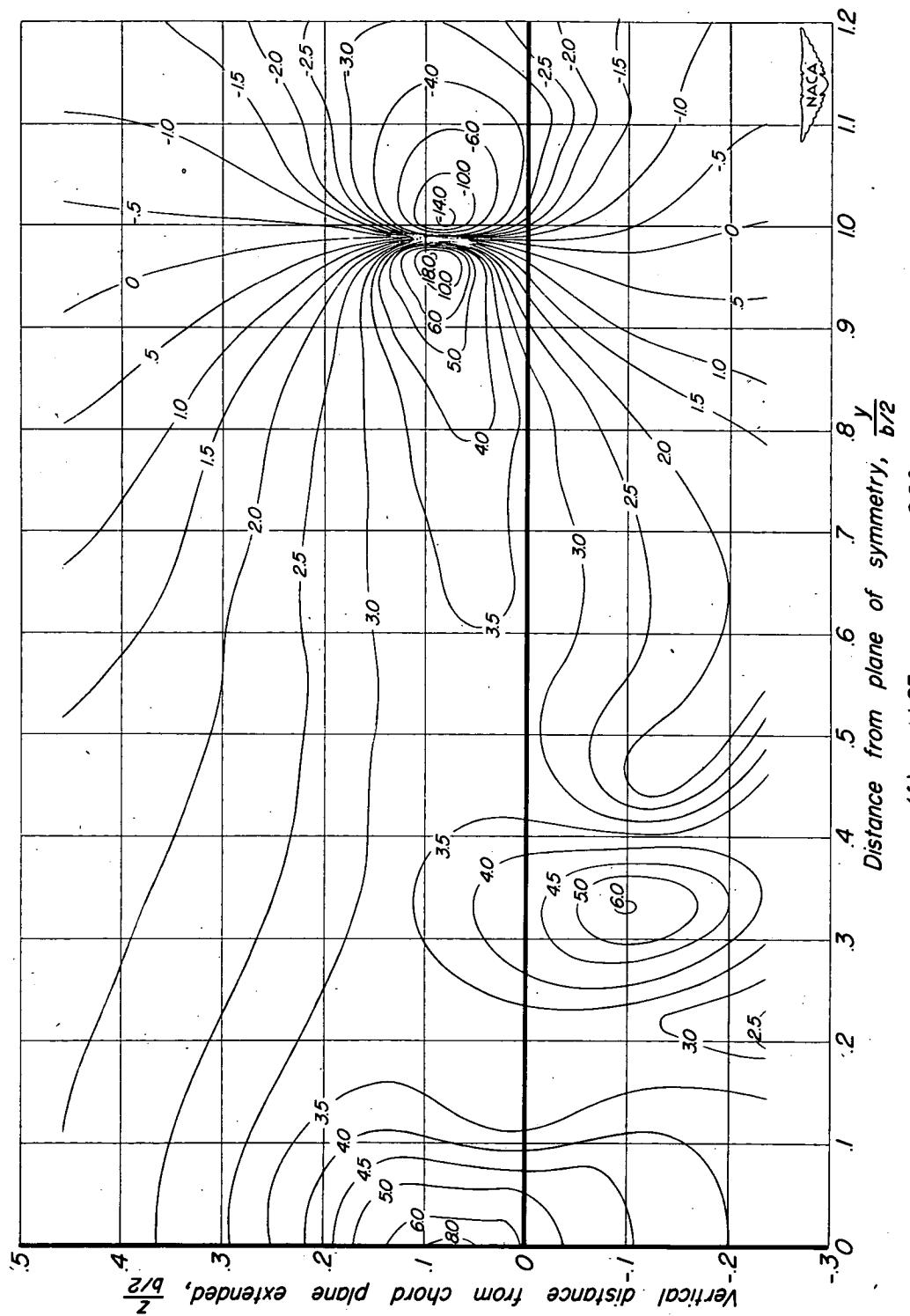
Distance from plane of symmetry, $\frac{y}{b/2}$

(f) $x = 1.65 \, b/2$, $a_{corr} = 6.9°$

Figure 6.— Continued.

Vertical distance from chord plane extended, $\frac{z}{b/2}$

(g) x = 2.00 b/2, a_{corr} = 7.2°

Figure 6.— Continued.

Distance from plane of symmetry, $\frac{y}{b/2}$

(h) $x = 2.36\ b/2$, $a_{corr} = 7.5°$

Figure 6.— Continued.

Vertical distance from chord plane extended, $\frac{z}{b/2}$

RESTRICTED   NACA RM A52J08
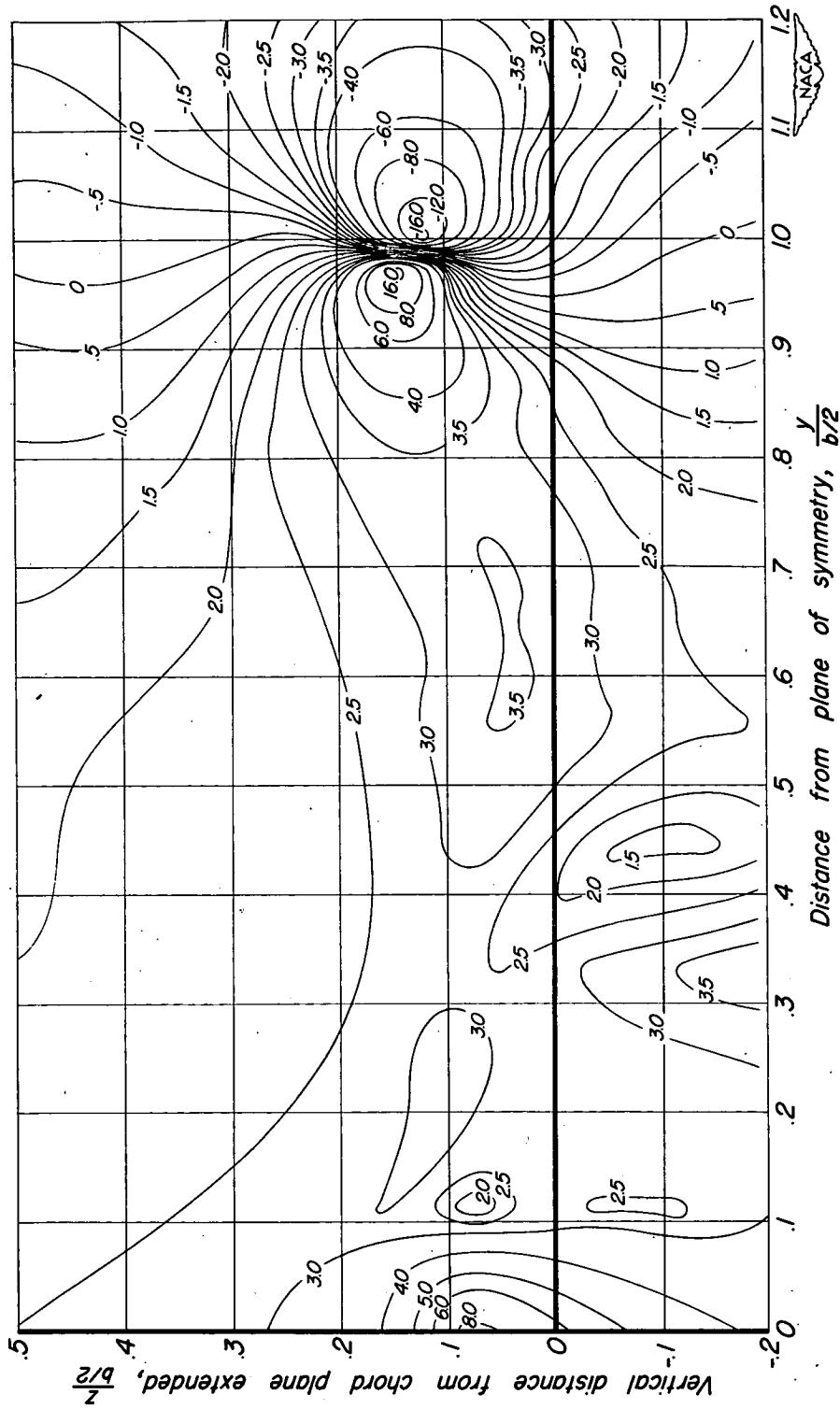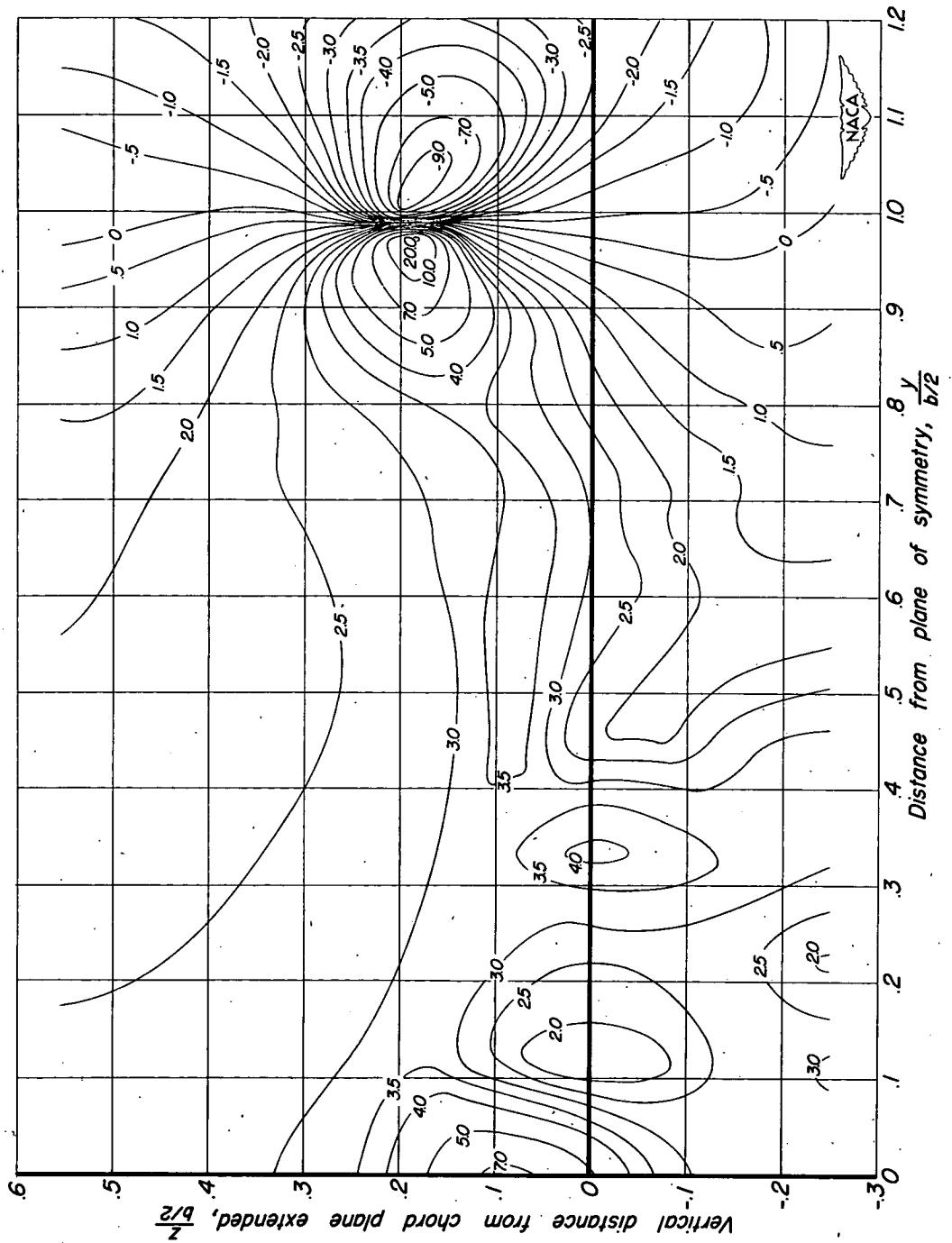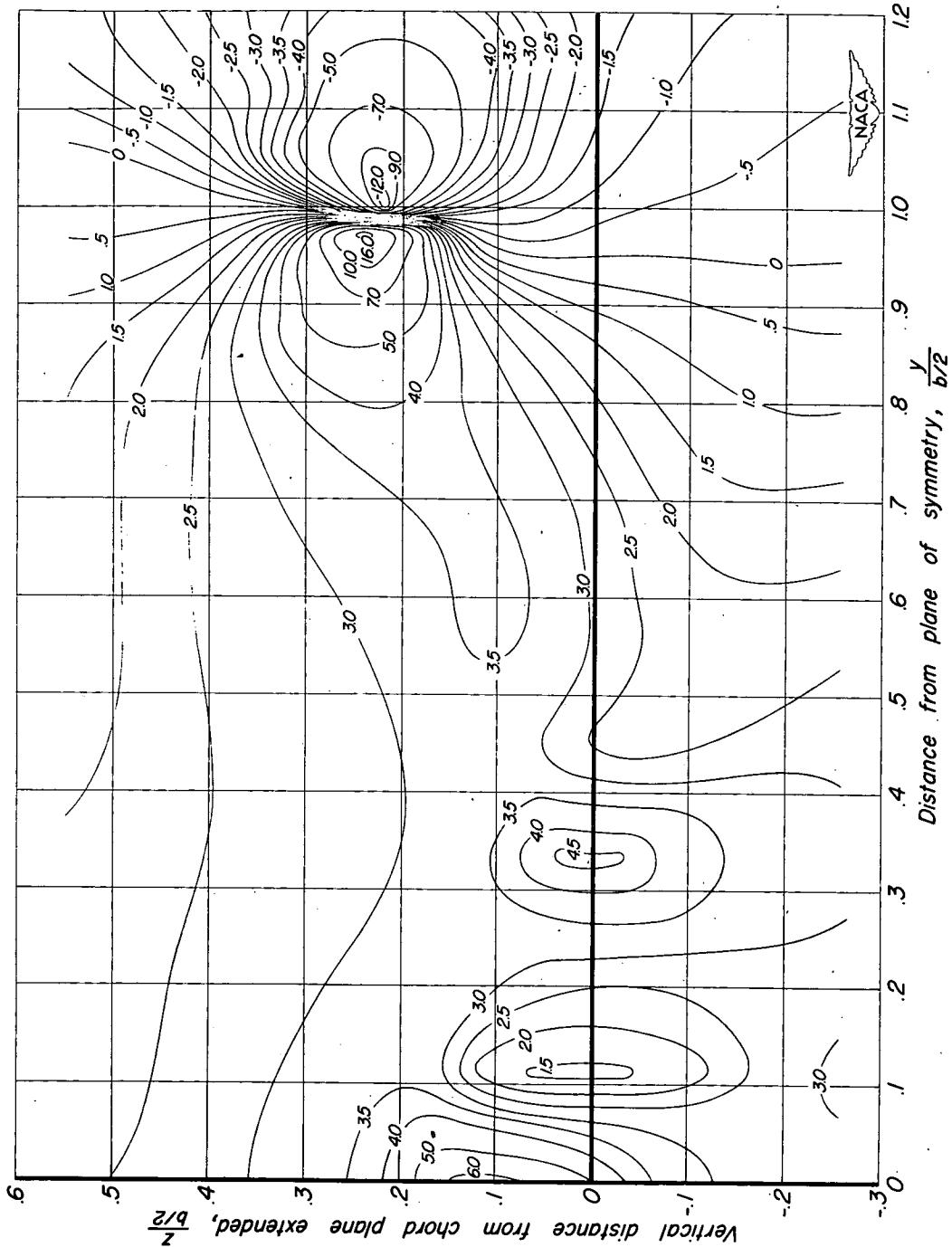
(i) $x = 2.71 \, b/2$, $\alpha_{corr} = 7.8°$

Figure 6.—Concluded.
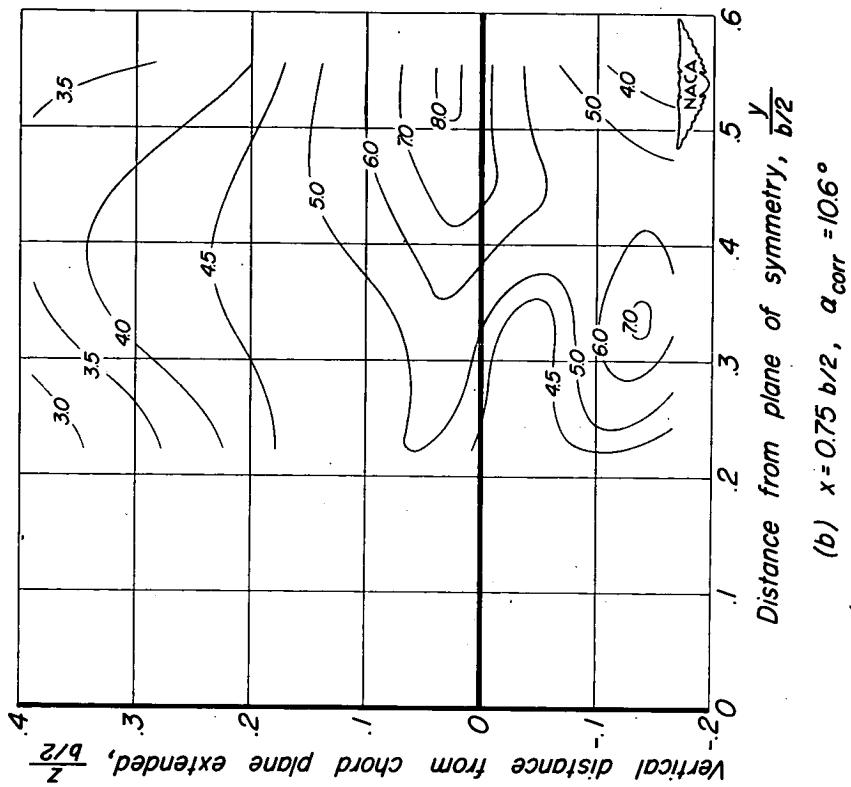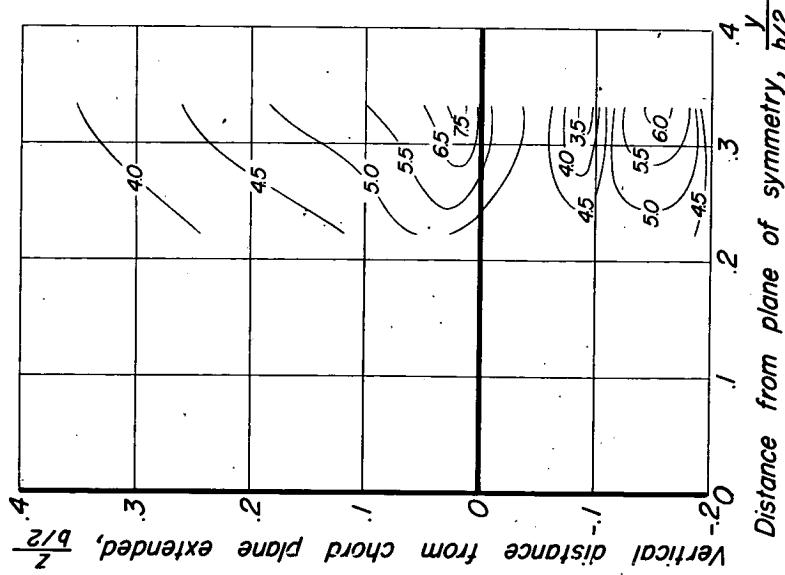
Figure 7.— Contours of constant downwash angles in vertical planes normal to the plane of symmetry behind the 63° swept-back wing-fuselage combination. $\alpha = 12.3°$.

(b) $x = 0.75\ b/2$, $\alpha_{corr} = 10.6°$

(a) $x = 0.57\ b/2$, $\alpha_{corr} = 10.5°$

(c) x = 0.96 b/2, a_{corr} = 10.8°
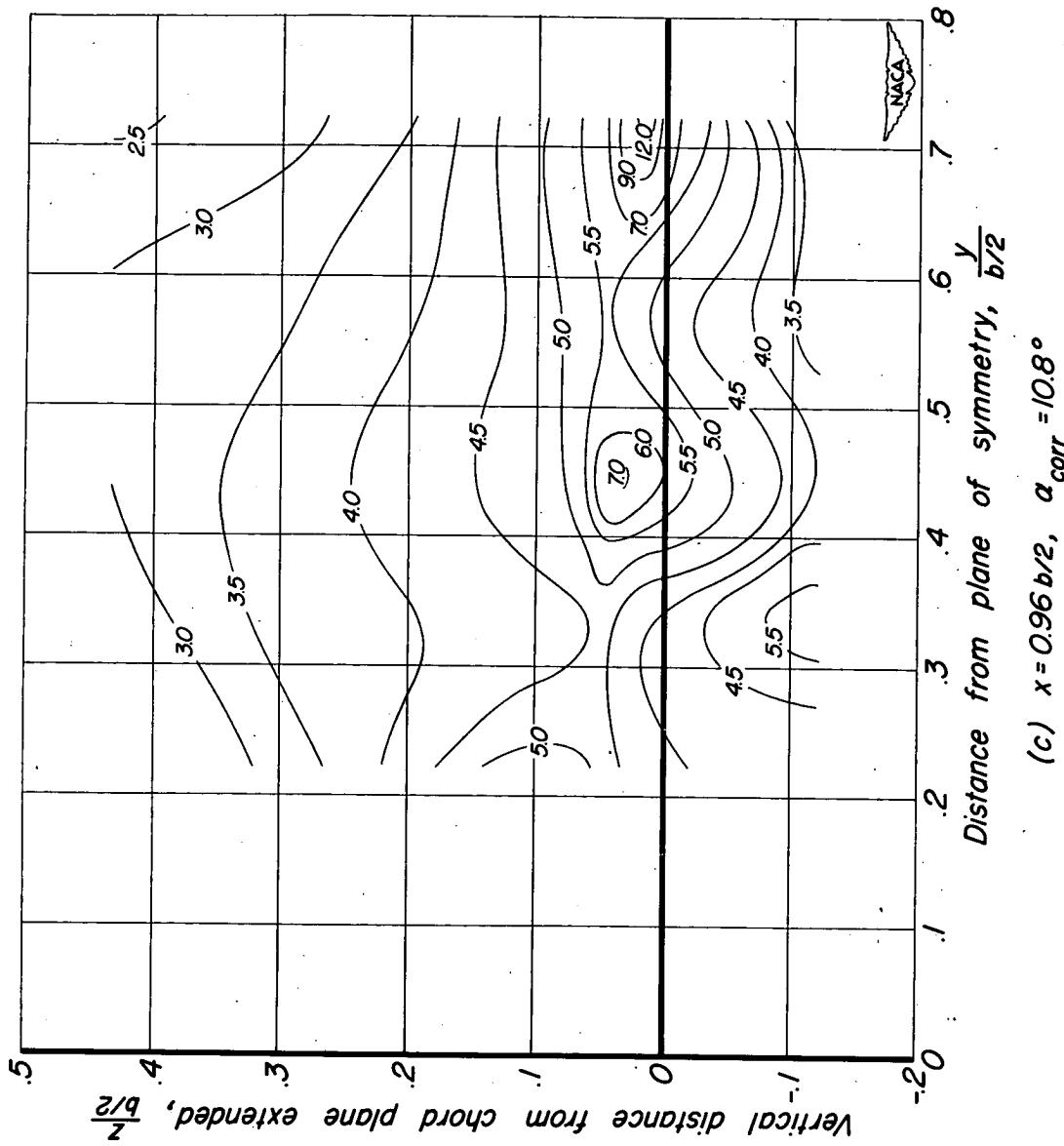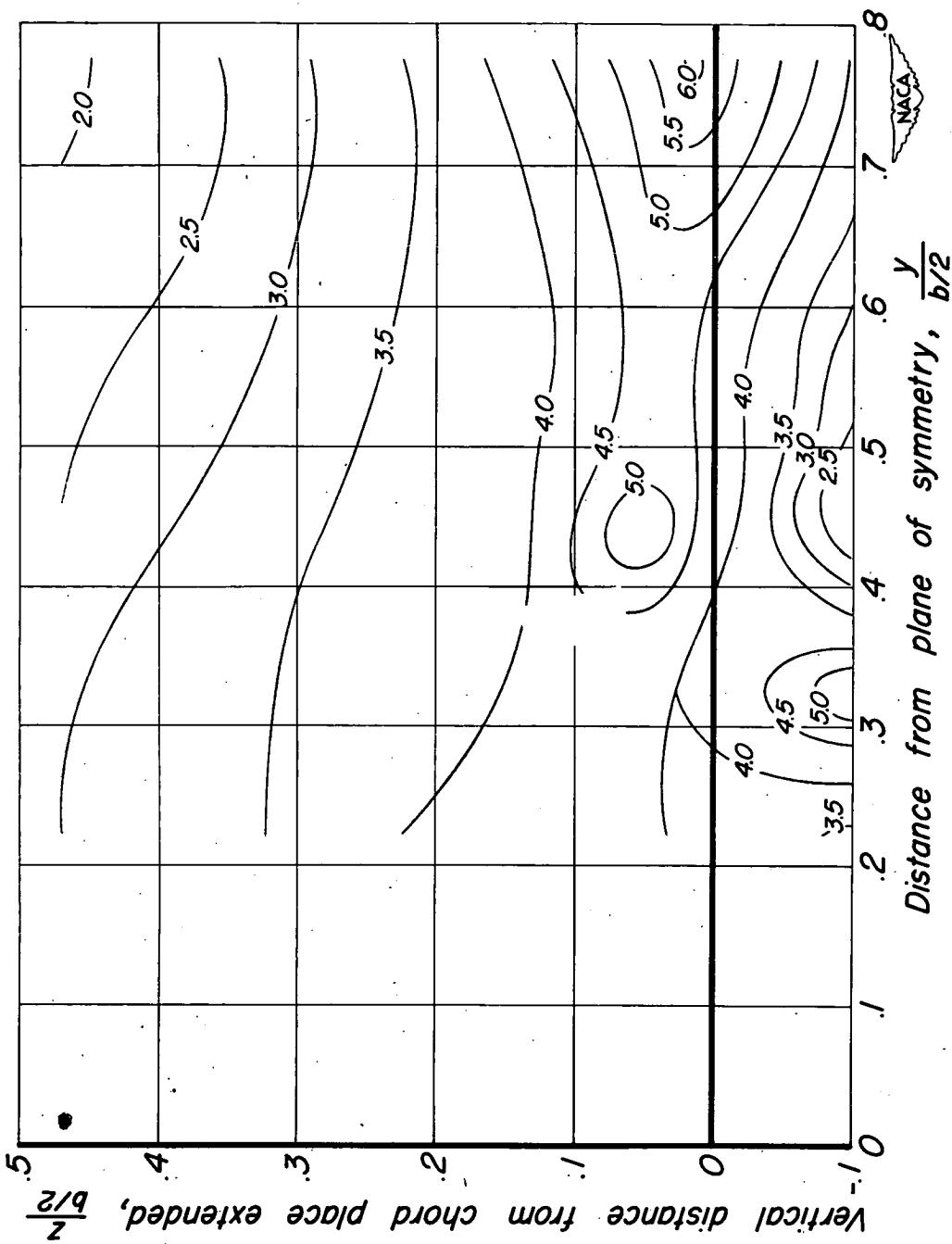
Figure 7.— Continued.

(d) $x = 1.11 \, b/2$, $\alpha_{corr} = 10.9°$

Figure 7.— Continued.

(e) $x = 1.31 \ b/2$, $a_{corr} = 11.0°$

Figure 7.— Continued.

Distance from plane of symmetry, $\frac{y}{b/2}$

(f) $x = 1.65\ b/2$, $\alpha_{corr} = 11.2°$
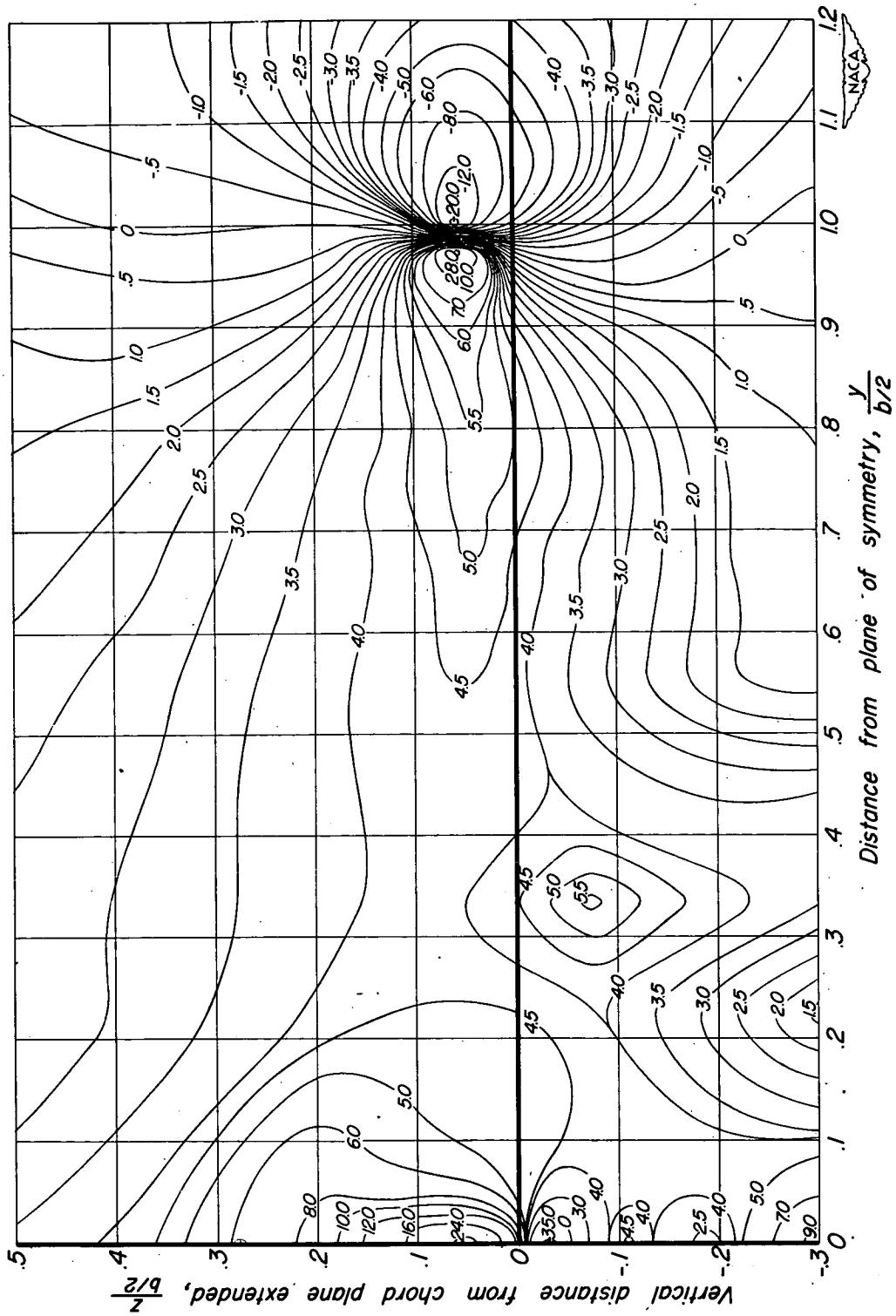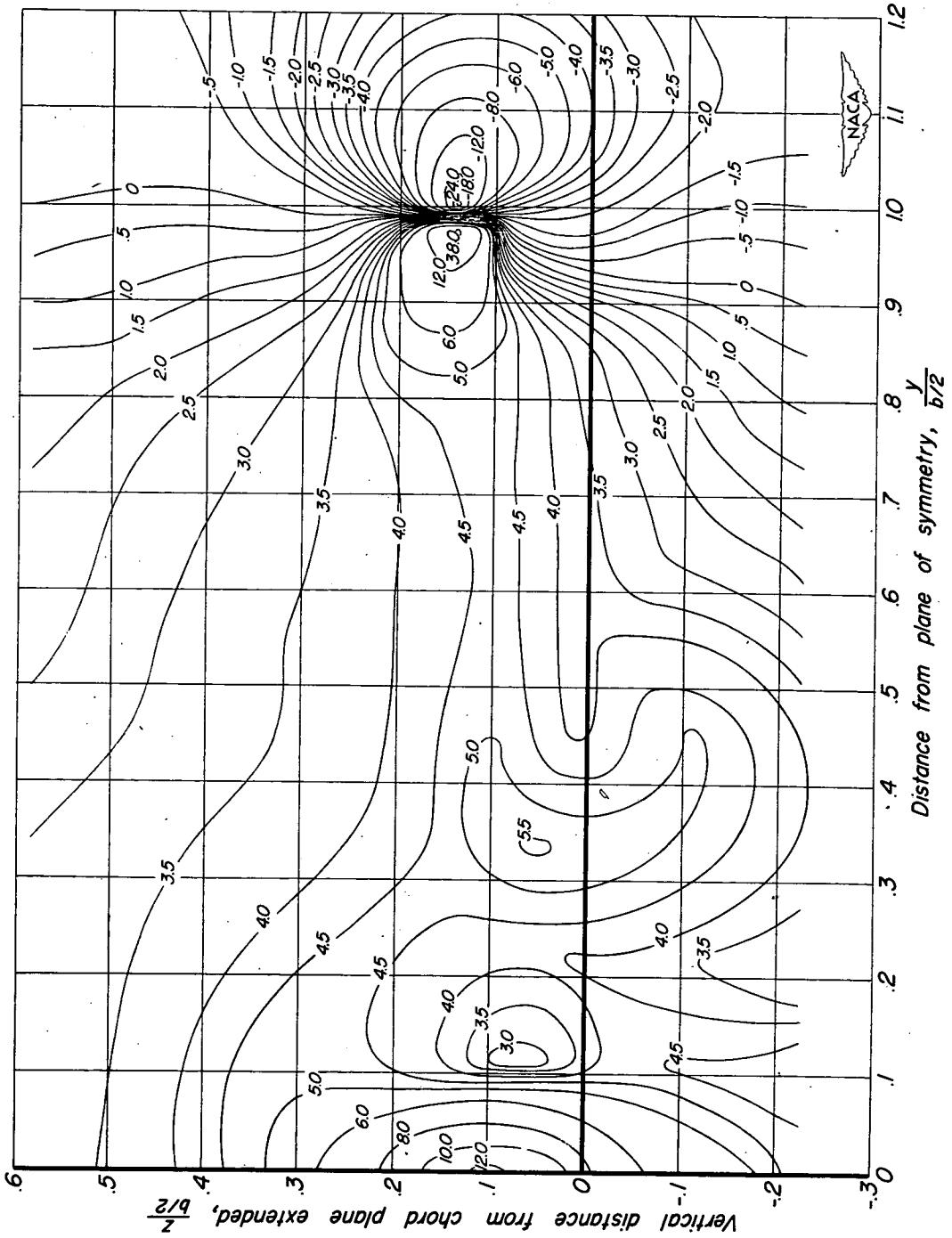
Figure 7.— Continued.
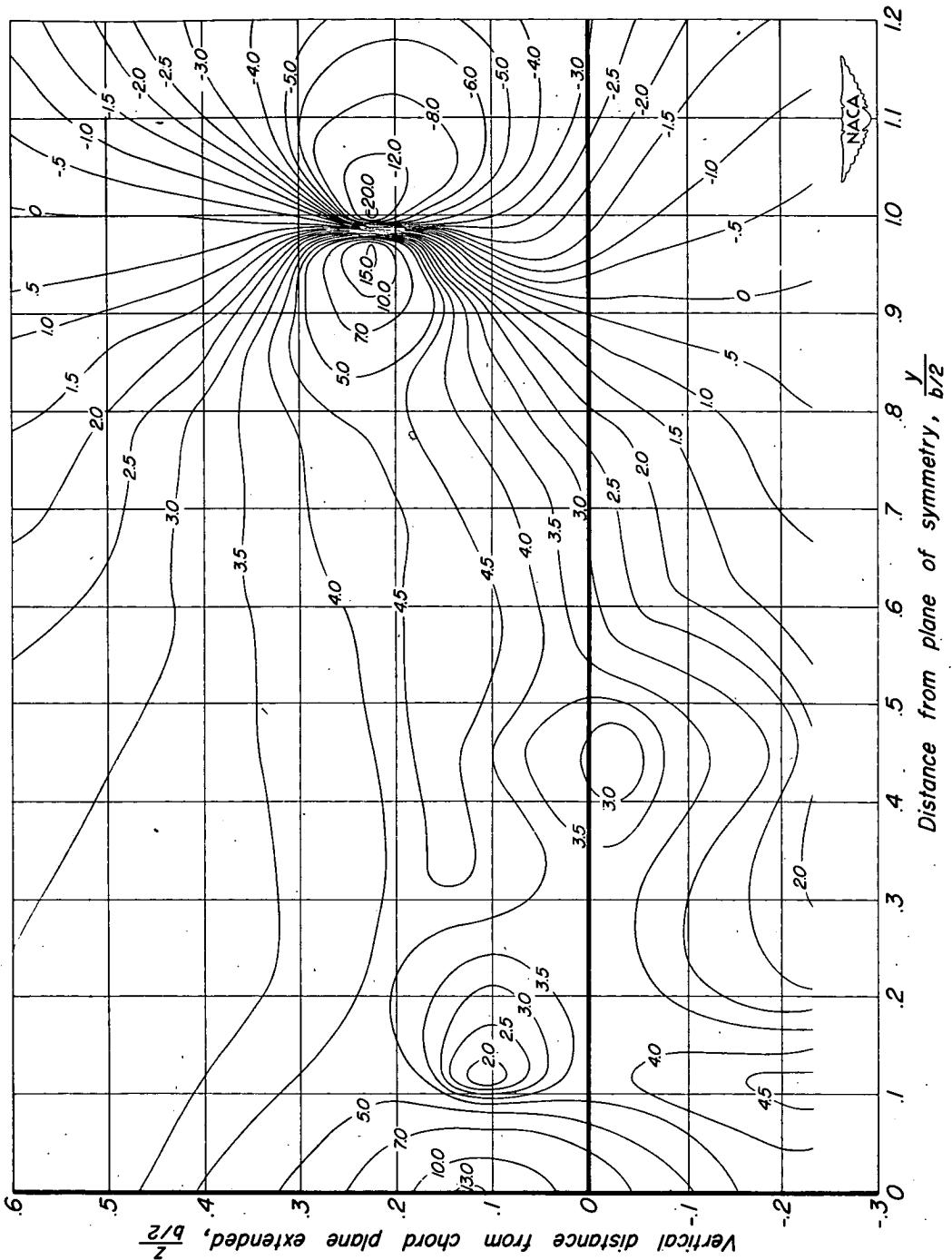
(g) x = 2.00 b/2, a_{corr} = 11.5°

Figure 7.—Continued.

Distance from plane of symmetry, $\frac{y}{b/2}$

(h) $x = 2.36\,b/2$, $\alpha_{corr} = 11.8°$

Figure 7.— Continued.

(i) $x = 2.71 \ b/2$, $\alpha_{corr} = 12.0°$
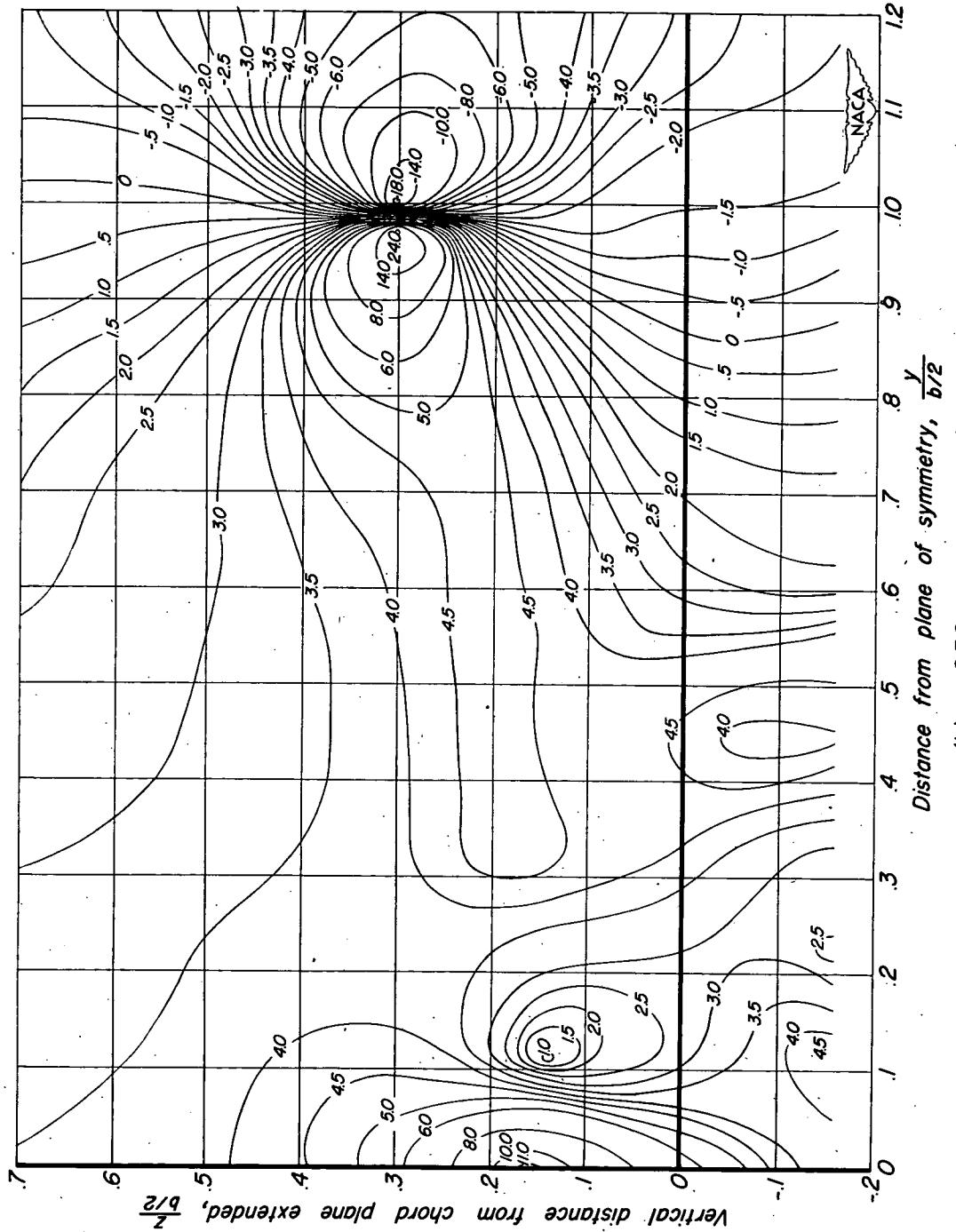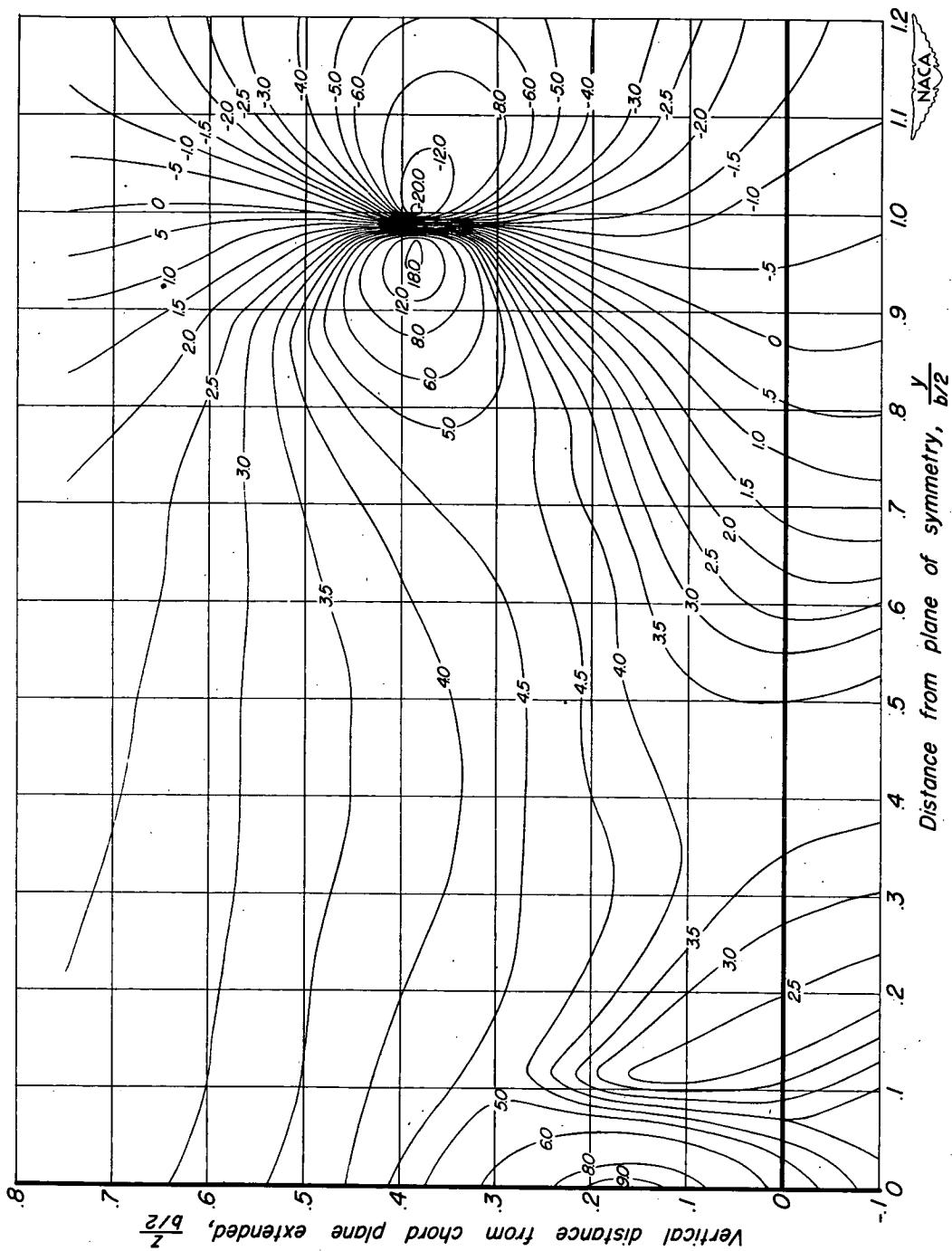
Figure 7.— Concluded.
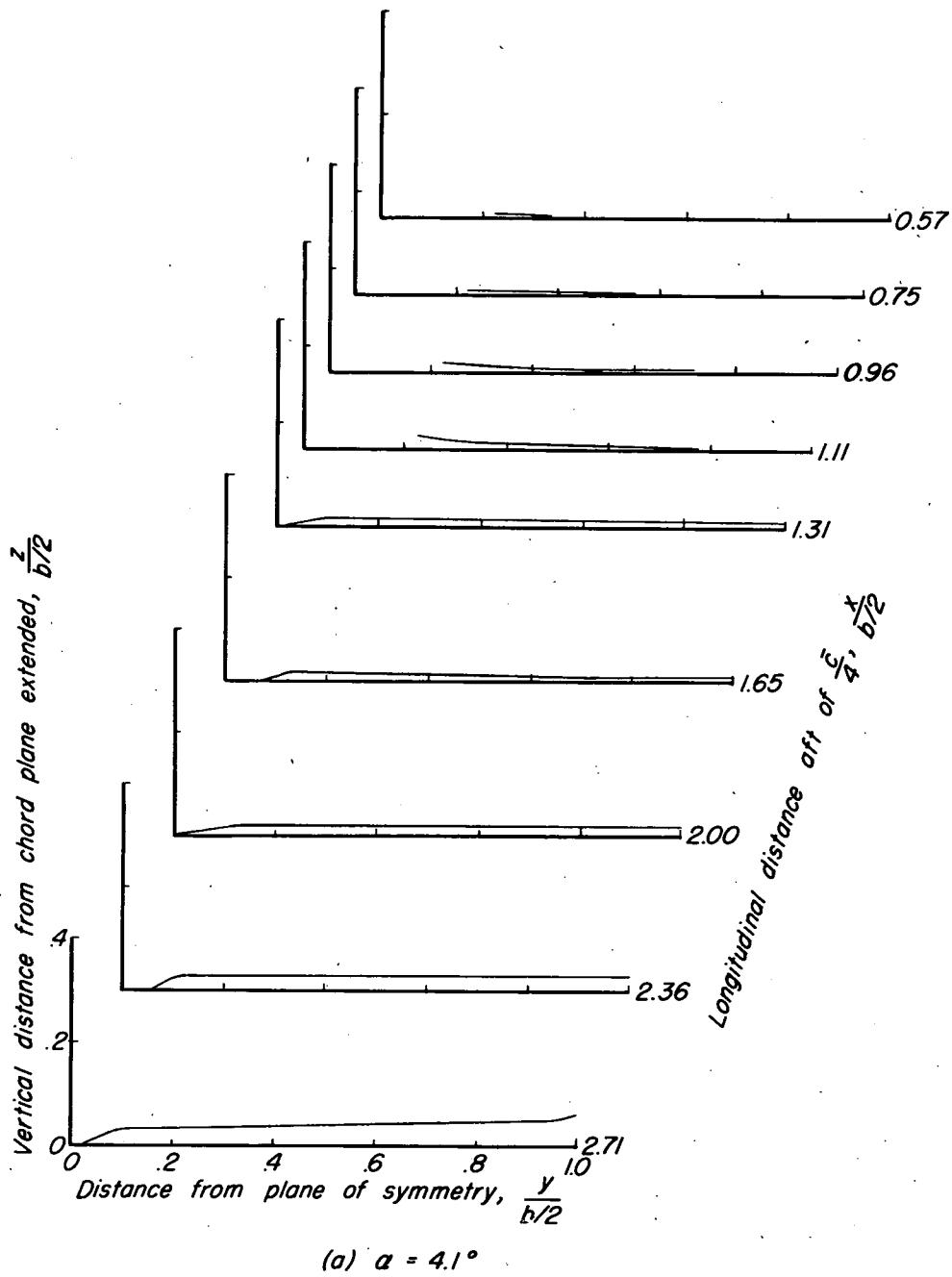
(a) $a = 4.1°$

Figure 8.— Vortex-sheet shape and position at various longitudinal distances aft of $\frac{\bar{c}}{4}$ of the 63° swept-back wing-fuselage combination.
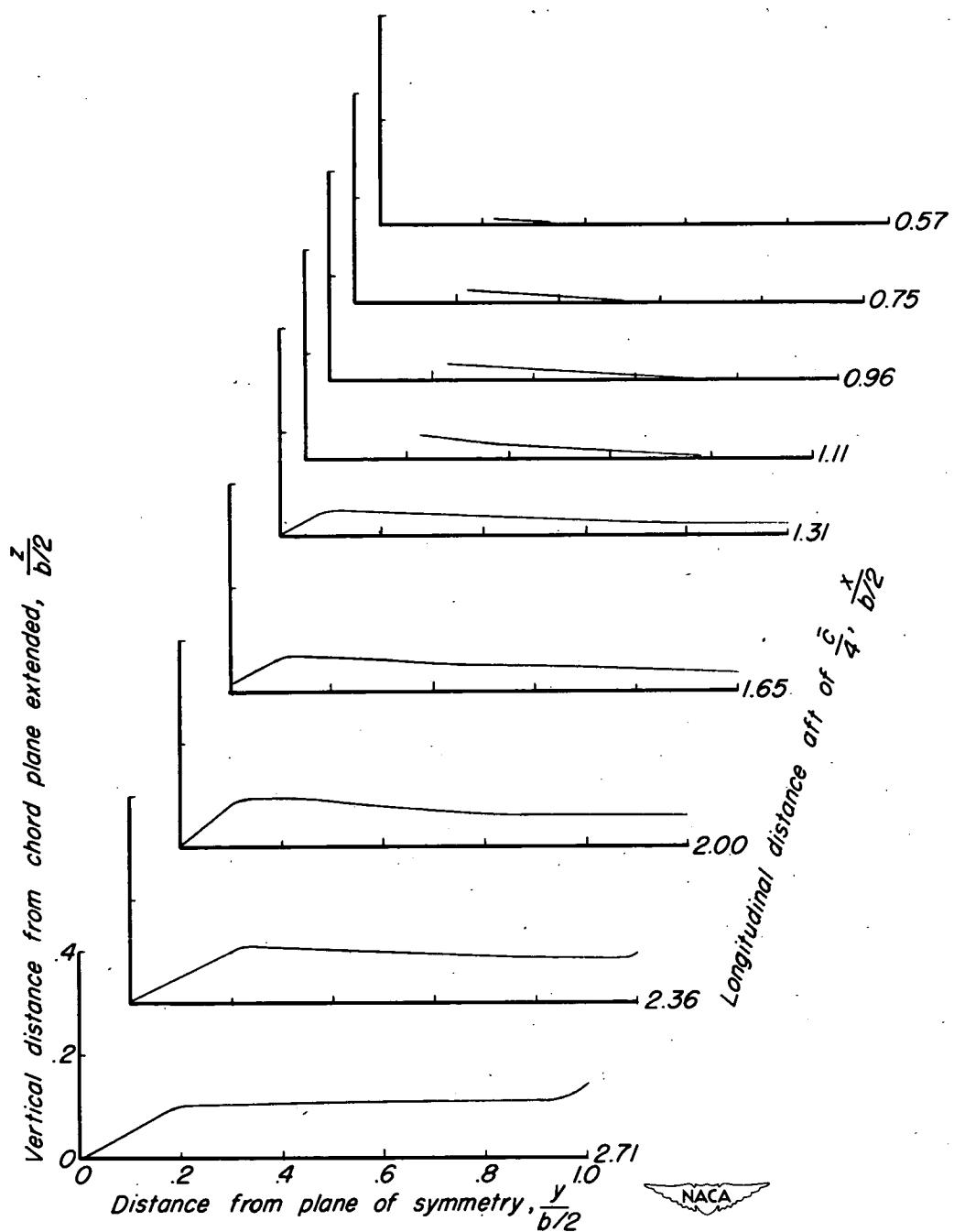
(b) $\alpha = 8.2°$

Figure 8 . — Continued.
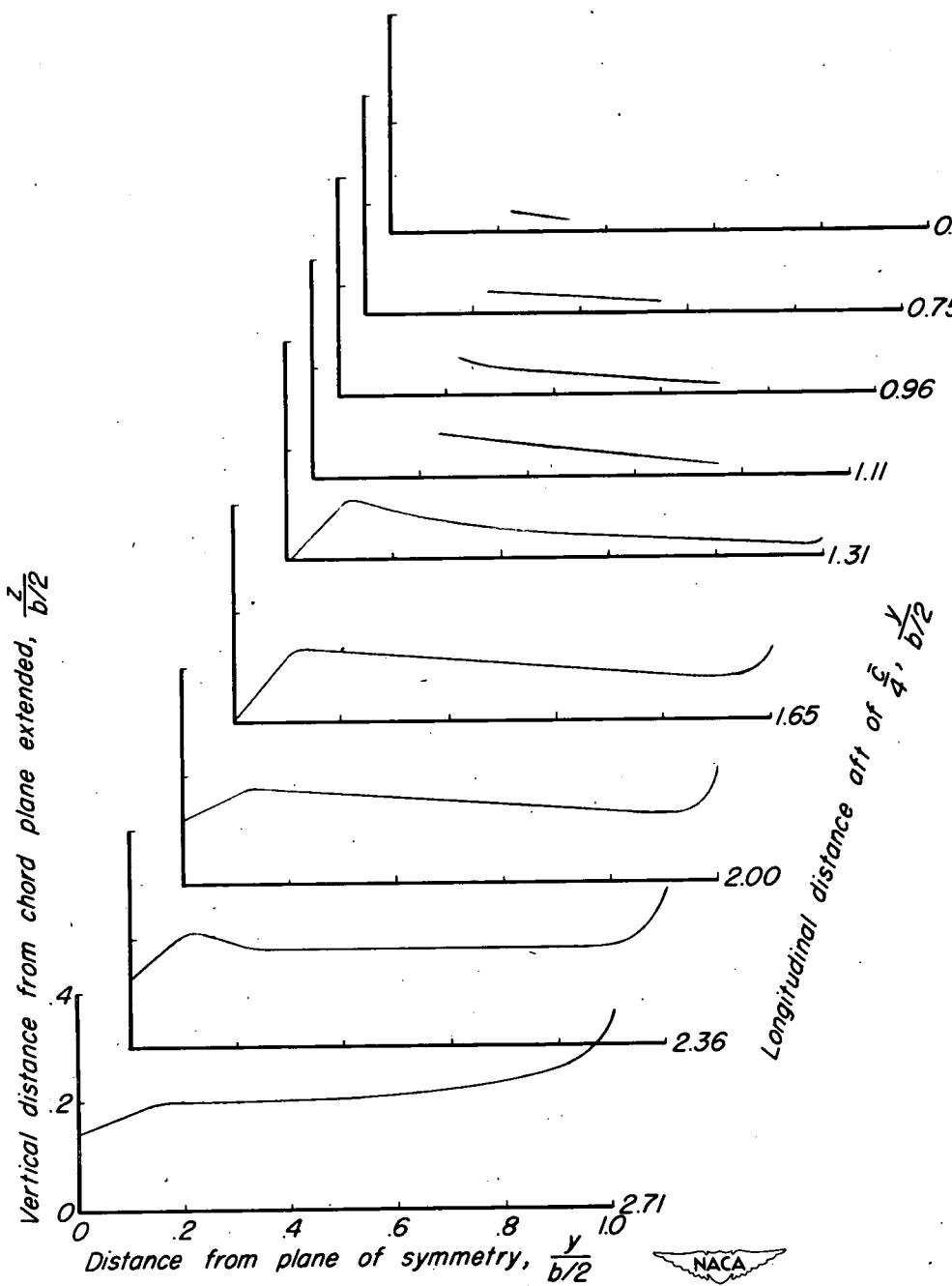
(c) $\alpha = 12.3°$

Figure 8 .— Concluded.
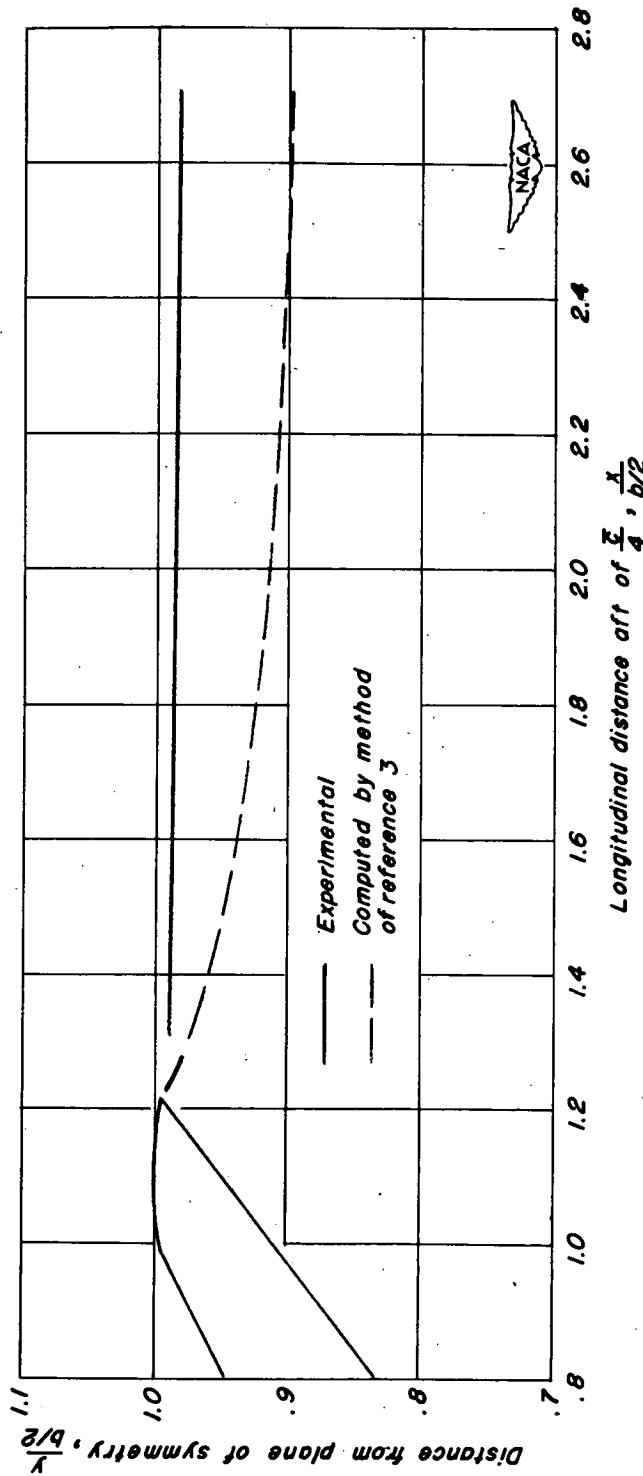
Figure 9.— Comparison of the experimental and computed tip vortex paths aft of the 63°

swept-back wing-fuselage combination at α =12.3°.
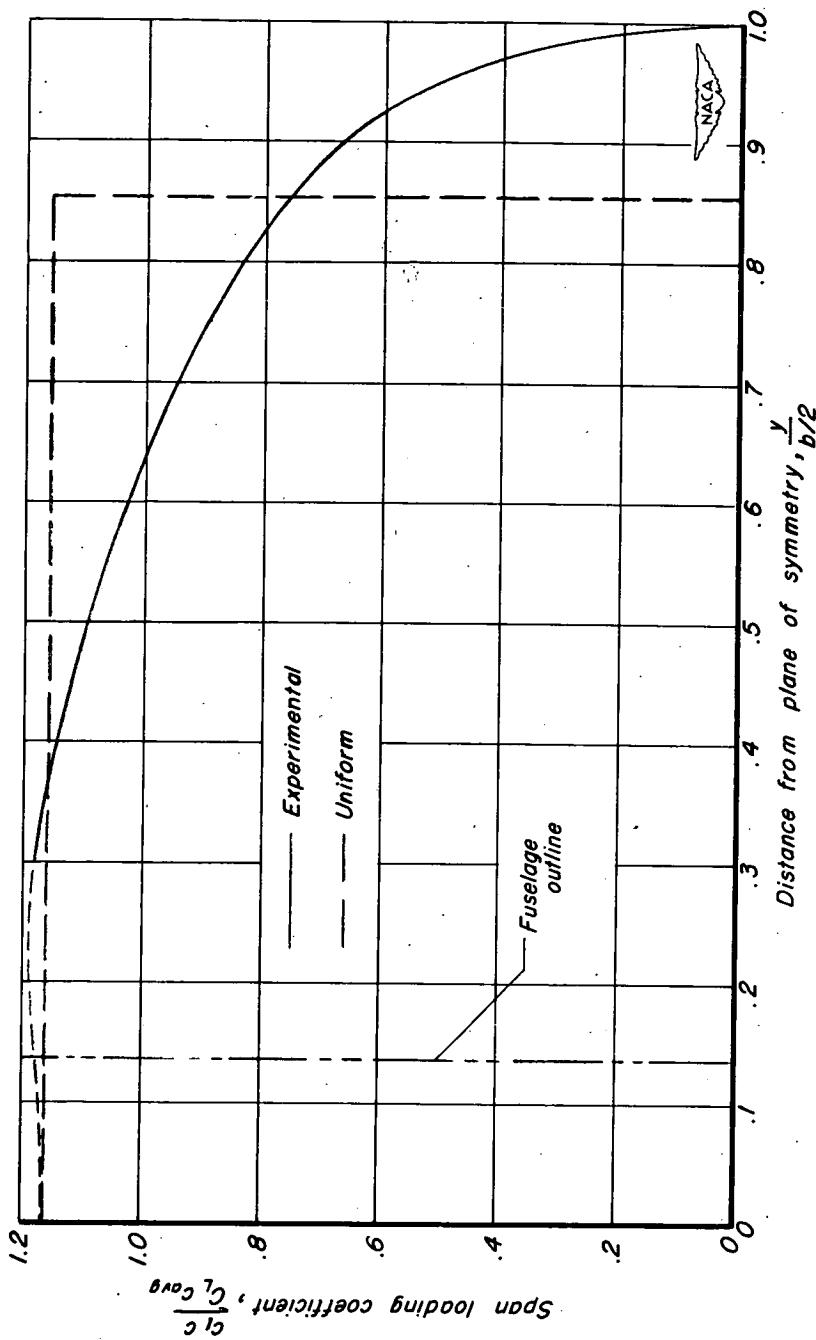
Figure 10.— Experimental and uniform span loadings used in computing the theoretical down-wash angles of the 63° swept-back wing-fuselage combination.
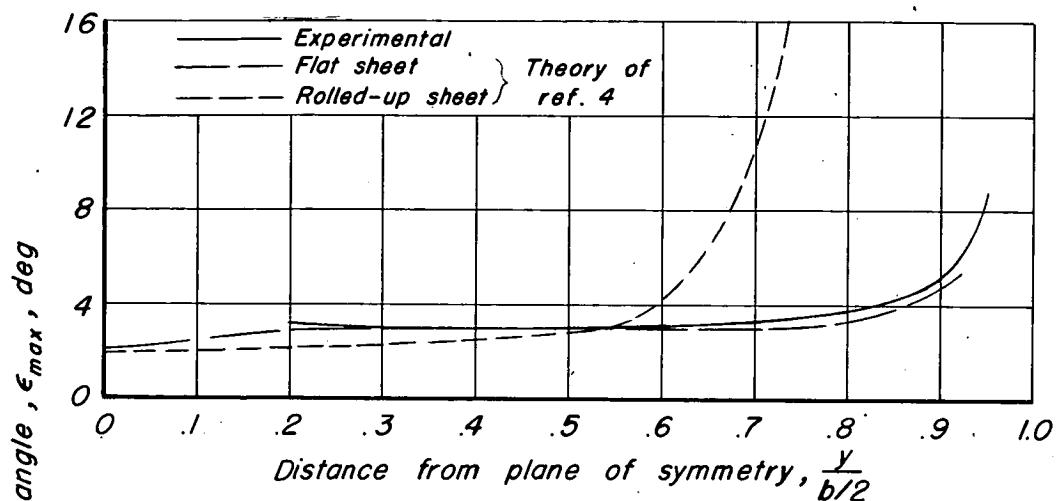
$x = 1.31 \ b/2$
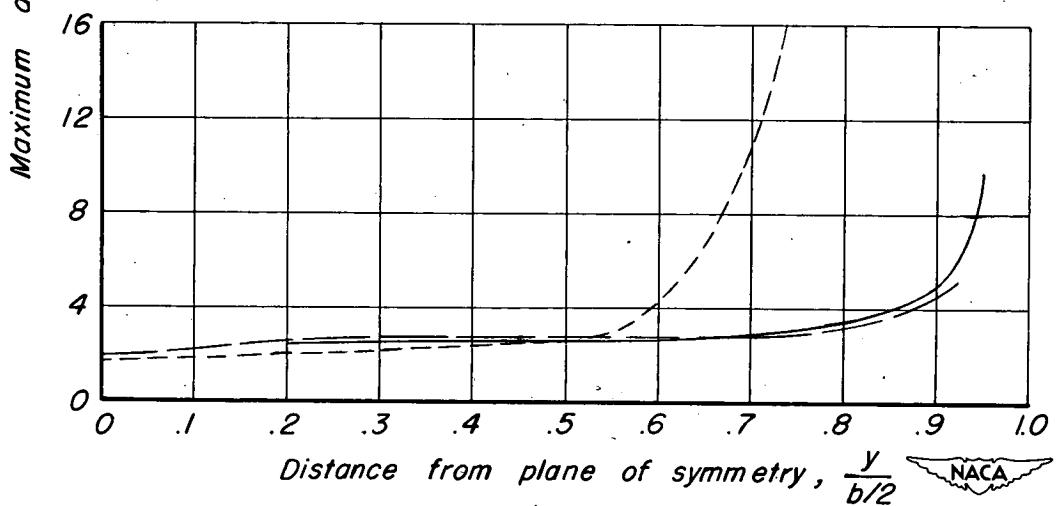
$x = 2.71 \ b/2$

(a) $\alpha_{corr} = 6.0°$ $C_L = 0.26$

Figure 11.- Comparison of the experimental and theoretical downwash distributions behind the 63° swept-back wing-fuselage combination.

Figure 11.— Concluded.